2009

The Synthesis and Characterization of Novel Elastin-Like Polypeptides Containing an Oligomerization Domain

James T. Cole
Cleveland State University

THE SYNTHESIS AND CHARACTERIZATION OF NOVEL ELASTIN LIKE POLYPEPTIDES CONTAINING AN OLIGOMERIZATION DOMAIN

JAMES T. COLE

Bachelor of Science in Biomedical Engineering

Case Western Reserve University

December 2005

submitted in partial fulfillment for the degree

Master of Science in Chemical Engineering

at the

Cleveland State University

May 2009

This thesis has been approved for the Department of Chemical and Biomedical Engineering and the College of Graduate Studies by

_____

Dr. Nolan B. Holland
Department of Chemical and Biomedical Engineering
Cleveland State University

_____

Date

_____

Dr. Orhan Talu
Department of Chemical and Biomedical Engineering
Cleveland State University

_____

Date

_____

Dr. Xue-Long Sun
Chemistry Department
Cleveland State University

_____

Date

ACKNOWLEDGMENTS

I would like to thank my academic advisor Dr. Nolan B. Holland for all of his support, help, patience and guidance during my studies. The advice and skills that he has helped me develop will no doubt be extremely helpful in the future for me. It has been a wonderful experience for me working in his laboratory and under his guidance.

I would like to thank Dr. Xue-Long Sun for allowing me to use his ultraviolet visible spectrophotometer as well as spending the time to be on my thesis defense committee. It is greatly appreciated. I would also like to thank Dr. Orhan Talu for taking the time to be on my committee, as well as the problem skills he helped me to develop during our advanced thermodynamics course.

My colleagues in Dr. Holland's laboratory have been of great assistance to me over the course of my studies. Ali Ghoorchian has been a valued friend and colleague from the beginning and has helped me to better understand our research and has always been there to listen to my ideas and provide valuable insight. Ozge Can taught me a great deal about life as well as being a great colleague and valuable scientific advisor. I will forever be grateful for his insights into a great number of topics.

Special thanks to Ms. Becky Laird and Darlene Montgomery for their support throughout my time at Cleveland State University. Ms. Laird has also guided me through many tough times by keeping me motivated and helping to see me through them.

Thanks to my father for providing me with the support and help throughout the years and finally, thanks to Ms. Stephanie Polites for giving me the motivation to restart my studies and to never stop striving to be a better man.

THE SYNYTHEIS AND CHARACTERIZATION OF NOVEL ELASTIN-LIKE POLYPEPTIDES CONTAINING AN OLIGOMERIZATION DOMAIN

JAMES COLE

ABSTRACT

Elastin like polypeptides (ELPs) are an emerging class of biomaterials due to their unique group of chemical, physical and biological properties. We have constructed a library of ELPs based on the pentapeptide amino acid repeat sequence (GVGVP). ELPs exhibit lower critical solution temperature (LCST) transition behavior from a soluble phase below the transition temperature (T_t) to an insoluble two phase system above the transition temperature. This process is completely reversible so that ELPs can become soluble again upon lowering the temperature. This temperature can be tuned in many different ways at the molecular level by changing the composition of the amino acid sequence and by changing the molecular weight of the ELP. Solution parameters such as ELP concentration and NaCl concentration can also change the T_t of the ELP and these effects were investigated. An oligomerization domain, named foldon, was attached to the library of ELPs and termed (GVGVP)-foldon. The T_t's of GVGVP and (GVGVP)-foldon were measured using ultraviolet spectrophotometry over a range of ELP concentrations, lengths and solution properties. The oligomerization domain is expected to reduce the T_t of the ELPs in comparison to linear ELPs due to increased chain length, molecular weight, hydrophobic interactions and intrinsic concentration. The trimerizing behavior of the foldon motif was confirmed by SDS-PAGE gel analysis. The results showed that the addition of the foldon domain reduced the T_t of all ELP constructs over a range of chain

lengths, ELP concentrations and solution parameters. However the effects of the foldon domain remain tied to the multi-variant effect that all ELPs show in regards to these factors. The ability to further alter the transitional properties of ELPs through the foldon domain increases our flexibility to make ELP constructs which are tunable to a wide range of desired transition temperatures.

TABLE OF CONTENTS

LIST OF FIGURES

CHAPTER I

INTRODUCTION

1.1 Introduction

Elastin-like polypeptides (ELPs) are one of a vast number of molecules that exist in nature which show specific functionality, self assembly capabilities and hierarchical organization. The properties of these molecules are derived from their amino acid sequences and monomer organization. Due to advances in molecular biology techniques and recombinant DNA technology it has become possible to create a wide range of materials based on specific amino acid sequences [1]. The synthesis of these synthetic genes leads to the production of genetically engineering protein based polymers (PBPs). PBPs will theoretically be able to demonstrate all of the properties that are present in the natural proteins that they are derived from. We are also able to construct PBPs that

exhibit functionality not seen in natural organisms due to the ability to create an almost limitless number of amino sequences that can encode the ELP gene.

In comparison to synthetic polymer synthesis the degree of control and complexity achievable in PBPs is far superior [2]. The general class of PBPs can be characterized as being mono-disperse and having molecular weights ranging from a hundred Daltons to more than hundreds of kDa's [3], which allows for the study of the materials dependence on molecular weight. Due to the fact that PBPs are based on the 20 naturally derived amino acids, the number of combinations possible is limitless.

1.2 Elastin-Like Polypeptides

Elastin-like polypeptides (ELPs) are considered the model system for the study and development of PBPs [4]. The basic structure of ELPs is a repeating sequence found in the mammalian elastic protein elastin [1]. The most common embodiment of this sequence is the pentapeptide, glycine-valine-glycine-valine-proline (GVGVP), which is found in cow and pig cross-linked elastin [5]. When cross-linked peptides composed of this sequence will replicate many of the mechanical properties of natural elastin. Early studies were performed on chemically synthesized poly(GVGVP), though recombinant DNA techniques are more widely used now. The combination of chemical, biological and physical properties found in GVGVP is beyond that of other PBPs and these properties are the subject of continued discovery and interest.

ELPs have amino acid side chains that are mainly aliphatic and hydrophobic. All ELPs show a reversible phase transitional behavior in response to temperature. This behavior is known as an inverse transition temperature (T_t) [6]. ELPs in solution below

their transition temperature are free polymer chains that are disordered random coils which can be characterized as being fully hydrated by hydrophobic hydration [7]. Above the transition temperature the chains undergo a process of hydrophobic folding and assembly. The end result of this is a distinct phase composed of 63% water and 37 % polymer [8]. The polymer chains in this folded state adopt a regular stabilized structure. The transitional behavior can be characterized by many different thermal methods, including turbidity measurements [4, 48, 58,68], nuclear magnetic resonance imaging [12,13,14,15,16], circular dichroism spectroscopy [17,18,48,58,68], Fourier transform infrared spectroscopy [19] and differential scanning calorimetry [20,56,57,62].

1.3 Advantages of ELPs

This section will briefly detail the many advantages that ELPs offer over conventional polymers. The ability to synthesize ELPs by either chemical methods or recombinant DNA techniques allows for either the rapid screening of many different constructs or the precise control of single constructs [4]. The ability to synthesize many different monomers, precisely control the amino acid sequence, stereochemistry and chain length gives the ability to design and synthesize proteins that are fine-tuned for desirable properties [48]. ELPs also have specific features that make them the model system for studying the principles of PBPs. ELP side chains are either the hydrogen atom or simple aliphatic groups which makes the properties of ELPs easier to interpret. The simplicity of the side chains also entails a lack of reactive side chains which enhances the stability over long periods of time and through different solution parameters. The unique transitional behavior of ELPs allows them to be used for many different applications.

1.4 Lower Critical Solution Temperature

The lower critical solution temperature (LCST) of a polymer is defined as the critical temperature and composition below which a mixture is miscible [9]. Above this temperature there is a distinct phase separation. This behavior is characteristic of exothermic mixing and negative excess entropy [9]. LCSTs are analogous to the inverse transition temperatures (T_t) that are a characteristic feature of ELPs. In ELPs raising the temperature above the LCST results in increased intramolecular and intermolecular order [7]. This process occurs by means of hydrophobic folding and assembly which can be described as the separation of the hydrophobic protein moieties from water [4].

1.5 Protein folding

In general, the folding of a protein is a physical process that transforms it into its native conformation, which is usually structurally stable and functionally active [11]. The conformation that is adapted after folding is dependent on the proteins amino acid sequence. The major stabilizing forces of a protein's overall conformation are hydrophobic interactions, electrostatic attractions and covalent linkages. Hydrophobic interactions are the most important stabilizing influence on protein native structures. The hydrophobic effect is the tendency of non-polar substances to come into minimal contact with polar solvents, such as water [21]. Proteins exhibiting this effect will fold in a way that non-polar residue side chains are buried in the proteins interior and away from the surrounding aqueous environment.

1.6 Temperature of Hydrophobic Folding and Assembly Transitions: Tt

The LCST of a polymer is essentially the same as the transition temperature (T_t) and thus the two terms will be used interchangeably in this study. The transition temperature (T_t) is the temperature at which hydrophobic folding and assembly transition occurs. The Gibbs free energy for a transition is zero and thus equations were developed to describe the T_t by Urry [4]. They are as follows:

$$\Delta G = \Delta H - T\Delta S \qquad \textbf{(2.1)}$$

Since the transition Gibbs free energy for a transition is zero;

$$\Delta H_t = T_t * \Delta S_t \qquad \textbf{(2.2)}$$

Rearranging and solving for the T_t leads to.

$$T_t = \Delta H_t / \Delta S_t \qquad \textbf{(2.3)}$$

The T_t is therefore a function of the differences in interactions of the water solvent and the residues of the ELPs. Urry defined the transition temperature by considering a multi-component system with one component within the system undergoing a decrease in entropy with an increase in temperature [6]. Urry also described the T_t as a measure of the hydrophobicity of the residues of a protein as well as a measure of the number of waters of hydrophobic hydration that change to bulk water during the transition [4].

Hydrophobic folding and assembly of ELPs can be described in the following manner. The phase transitional behavior of ELPs can be seen in figure 1.1 and 1.2, which is a demonstration of ELP below and above the transition temperature. Below the T_t the ELP is soluble in water and upon raising the temperature there is a clean phase separation

with aggregation of the ELP occurring. In the unfolded state the disordered free polymer chains of the ELP are fully hydrated by waters of hydrophobic hydration [1]. Hydrophobic hydration can be described as cage-like water structures surrounding the hydrophobic groups of the ELP [4]. These waters have thermodynamic properties of having decreased enthalpy and entropy in comparison to the bulk water surrounding the ELP. Water molecules surround the ELP and interact via van der Waals interactions. The water molecules arrange themselves around the ELP in this manner because it allows them to maintain hydrogen bonding between themselves. The cage like structures of water avoids the loss of most of the hydrogen bonds and this places the water in a favorable energetic state. This maximizes the van der Waals contacts between the hydrophobic solute and the water but does not reduce the hydrogen bonding. These structures are easily disrupted by raising the temperature [21].

Figures 1.1 and 1.2: Images of ELPs produced in the lab at temperatures below the LCST (LEFT- clear liquid) and above the LCST (Right- turbid solution).

The most common description of the secondary structure of GVGVP in the folded state has been determined by the work of Urry and his group to be a β-spiral, which is shown in figure 1.3. This structure is stabilized by intra-spiral, inter-spiral and inter-turn

hydrophobic contacts with the main secondary feature being a β-turn [7]. The presence of β-turns or β-sheet-like secondary structure has been reported by circular dichroism spectroscopy in numerous studies [48,58,63].

Above the T_t there is a destruction of the ordered water structures of hydrophobic hydration surrounding the polymer chain [4]. The cage like water becomes less ordered bulk water and the hydrophobic side chains begin to associate with each other, which increases the order of the ELP. The folded chains take on the form of a regular dynamic pattern, with type II β-turns as the main secondary structure which eventually form into β-spirals that are stabilized by intra-spiral, inter-turn and inter-spiral hydrophobic contacts. As more waters transition from hydrophobic hydration to bulk water and the system further dehydrates, the β-spirals hydrophobically associate and take on the form of fibers. These fibers begin to form filaments that are composed of triple-stranded β-spirals that grow to several hundred nano-meters length. The β-spiral structure is further stabilized by these triple helices. The contour length of this folded state is $1/5^{th}$ the length of the unfolded polypeptide. Eventually the triple-stranded ELPs settle into an aggregated phase-separated state. The process of dehydration, chain-folding and phase separation is completely reversible and as the temperature is dropped below the T_t the system returns to its original state.

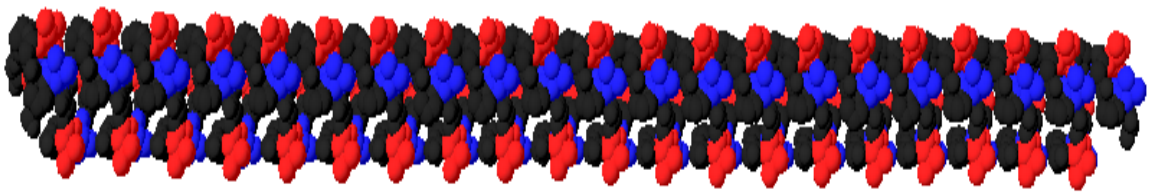

Figure 1.3. GVGVP triple strands composed of β-spiral structures

1.7 Alternative Descriptions and Studies on the Secondary Structure

Despite the widely regarded views of Urry, the secondary structure of ELPs has been a point of debate and other researchers have investigated the secondary structure of ELPs above their T_t. The findings have shown that despite the aggregational abilities of ELPs they do not have a well-defined folded three dimensional structure. Recent experiments utilizing nuclear magnetic resonance spectroscopy (NMR) have been performed to determine exact structural elements [12,13,14,15,16]. The Cabello group investigated two ELPs, poly(GVGVP) and poly(AVGVP), in water using NMR spectroscopy [12]. The results showed that there were 4 distinct physical states in different temperature regions. The first state was below the T_t and was rather extended, statistically shaped and fully hydrated. The second state was coiled and globular but not well-defined. For GVGVP this region extended into the 3rd state which was a more tightly coiled and compact state above the T_t. The final state was well beyond the T_t and constituted an aggregated and flocculated state. States 2 and 3 were shown to lose some of their hydration, but retained immobilized water molecules in the coils. In the second state there was no distinct recognition of β-structures, but there was indication of a more coiled environment.

A second NMR study was performed by the same group using the structure $[(GVGVP)_2\text{-}(GEGVP)\text{-}(GVGVP)_2]$ at two different chain lengths [13]. The results showed the following interesting conclusions. The first was that there was an increase in rigidity of the ELP at and above its T_t. This stiffening is derived from the backbone and ELP coiling and aggregation follows the stiffening. The second observation of note was

that the conformational behavior of the visible parts of the ELPs did not differ from that of random coils both above and below the T_t.

Molecular simulations have been employed to attempt to determine the mechanism of the T_t behavior of ELPs [22,23,24]. An ELP, $(GVGVP)_{18}$ was used in simulations by Li. et al. [22] at temperatures above and below the T_t. Results showed that the waters of hydrophobic hydration played a major role in the elasticity of ELPs. These results call into question Urry's description of the elastomeric restoring force resulting from the reduction of librational entropy as β-turns are stretched.

The conformational behavior of poly(GVGVP) was studied by Krukau et al. using computer simulations in a temperature range above and below the T_t [22]. They were able to distinguish two main conformational states of the ELP. The first was a rigid conformational state at low temperatures and the second was a flexible state at higher temperatures. There was a distinct transition between the two states. The transition indicated the disruption of the waters of hydrophobic hydration. There was an indication of a random distribution of end-to-end distance at the high temperature states which indicated a random coil structure. However they also were able to detect the presence of various structural elements. These structural elements though were located at irregular or random points along the chain and there was frequent inter-conversion between them. The final conclusion is that there are ordered structural elements present in the ELP but they are distributed randomly and there is no indication of a definitive secondary structure such as a β-spiral. Another molecular dynamics study was undertaken by Baer et al. [23] that showed that above the T_t there was an increase in the number of folded structures of the ELP but there was no direct indication of the nature of these structures

The Cabello group investigated the solid state of ELPs using vibrational Raman analysis and thermal wide range X-ray diffraction techniques [25,26] . The findings indicated that the solid state was composed of a meta-stable amorphous phase composed of polymer chains without definitive order [25]. The only structural feature that could be distinguished was a net of hydrogen bonds that comprised the majority of the amide groups. Raising the temperature caused the hydrogen bonds to break and the chains to reorganize into a non-crystalline state. The same group used FTIR analysis as well as Raman spectroscopy to investigate the structural changes of poly(GVGVP) and poly(AVGVP) [19]. Below the T_t, part of the amide groups interacted with neighboring water molecules while the other part interacted with each other to form β-sheet like structures. Also it was seen below the T_t that the water shells were more closely structured around the ELP. Finally they observed that the more hydrophobic ELP, poly(AVGVP) formed a more compact suspension above its LCST and was more difficult to return to its non-aggregated state.

1.8 Variation of the Transition Temperature

One of the greatest features of ELPs is the ability to alter the transition temperature based on a host of factors. These factors include chain length, polymer concentration, polymer composition, solution composition, pH, side chain charge and light. In this study we will investigate the effects of chain length, polymer concentration and solution composition. However some of the other effects will be briefly discussed here. The functionality of $(GVGVP)_n$ will be maintained as long as the glycine and proline residues are left in place, which leads to the ability to substitute at the following

positions: poly (GαGβP)n. The α position can be filled with any of the 20 natural amino acids. The β position can also be replaced with any of the natural amino acids, except for proline due to the nature of the formation of β-turns between glycine and proline residues. Changing the polarity or the hydrophobicity of the ELP will change the T_t. Urry was able to develop a T_t -based hydrophobicity scale which charted the effects of substituted amino acids under common solvent conditions [4]. The end results of this scale was that the more hydrophobic the substitution was the more it depressed the T_t and the higher the values of T_t were indicative of more polar side chains.

ELPs are also pH responsive and this relates to the idea that the T_t of all ELPs depends on the mean polarity of the polymer [34]. An ELP with glutamic acid (E) in the substitutable position was studied [Girotti 2004]. The γ-carboxylic group of E showed large polarity changes when the pH changes between the protonated and deprotonated states. At a pH of 2.5 the T_t was found to be 28 °C and at a pH of 8.0 the T_t was 85 °C. The design of this ELP contained just 4 glutamic acid residues per 100 amino acids in the polymer backbone, which was enough to affect a difference of 57 °C in the T_t between pH states.

1.9 Aim of the Thesis

The main goal of this work is to understand how to fully synthesize and characterize novel elastin-like polypeptide constructs which contain an attached oligomerization domain. Common molecular biology techniques as well as recursive directional ligation were used to synthesize all of the ELPs. Novel ELP constructs were created through the addition of an oligomerization domain to the synthesized ELPs. This was done using similar molecular biology techniques and all of the constructs were

expressed in *E. coli*. The purpose of this addition was to attempt to control and improve the rate of ELP chain assembly as well as alter the thermal transition behavior of the constructs. Constructs containing the oligomerization domain were compared to the constructs lacking the domain to determine the differences in transitional behavior, concentration dependence and chain length dependence. Theory has shown that ELPs are strongly concentration dependent while studies involving the oligomerization domains have shown that it was possible that constructs containing the oligomerization domain may be rendered concentration independent. The addition of the oligomerization domain also has other advantages. By essentially tripling the size of our ELPs we should be able to see behavior that is similar to linear ELPs of similar size to the foldon induced trimers and thus we should be able reduce the T_t of shorter ELPs. Constructs of varying chain length were synthesized and the dependence of the transitional behavior was investigated. Finally solution parameters such as the addition of NaCl have been known to alter the transitional behavior of ELP constructs and these effects were observed.

The addition of the oligomerization domain should impart the advantages that the foldon domain offers to ELPs. Those include reducing the T_t, trimerizing potential, higher intrinsic concentration and increased thermal stability. Another advantage of the oligomerization domain is the ability to rapidly expand the size and variability of our library of ELPs. By understanding how to synthesize the different types of ELP constructs and the different factors that alter their transitional behavior we move closer to being able to design an extremely wide range of ELPs tunable to any set of desired conditions.

Chapter II

Background Information

This section will introduce relevant background information to this study. Topics to be covered include applications of ELPs, relevant molecular biology information, oligomerization domains and the effects of different factors on the LCST of ELPs.

2.1 Applications of Elastin-Like Polypeptides

This section will detail some of the current applications of ELPs in biomedicine and technology. Due to their tunable T_t, biocompatibility and precise control of molecular weight, sequence and chain length, ELPs are useful for a wide variety of biomedical applications [27]. ELPs are promising for future use in "smart" devices in many fields such as nanotechnology, biomaterials science, organic chemistry and biochemistry [28, 29]. Currently the common applications of ELPs include tissue engineering, drug delivery, protein purification, biosensors and hydrogels.

2.2 ELPs in Tissue Engineering

The use of ELPs for in biomedical technology is mainly in the field of using biocompatible polymers as tissue engineering and tissue repair scaffolds. Due to their integration into the body, the design of tissue engineering scaffolds is not trivial and is dependent on a wide range of factors. The scaffold must be biocompatible, biodegradable, be able to exist in physiological conditions and should promote cell-substrate interactions. ELPs have generally been considered to be biocompatible due to the fact that they are based on naturally derived amino sequences, but these findings were not confirmed until Urry et al performed a study in 1991 [30]. The confirmation came from performing the entire series of recommended generic biological tests for materials to be placed inside the body. The use of standard poly(GVGVP)$_n$ as a cross-linked matrix showed no cell adhesion [31]. The addition of other functional groups to GVGVP, including the amino acid sequence arganine, glycine and aspartic acid (RGD) created more active cell-binding sites [32].

The Chilkoti group [33] investigated the rheological behavior of ELPs to determine their suitability for use in cartilaginous tissue repair [33]. They found that the complex shear modulus of the ELP increased by 3 orders of magnitude during phase transition using a displacement controlled rheometer. These observed values were similar to the values previously reported for collage, hyaluronan and synthetic hydrogels. Chondrocytes were cultured in an ELP solution and characterization studies showed that these cultured cells maintained their characteristics and showed the synthesis of a large

amount of extracellular matrix materials. The combination of the two results indicated the great potential for ELPs to be used for forming scaffolds for cartilaginous tissue repair.

Giroti et al. combined four different functional domains in an ELP monomer in order to mimic the characteristics of the extracellular matrix (ECM) [34]. The main goal was to show a mechanical response comparable to the ECM, which was achieved by using the repeat sequence (VPGIG) as the base building block. The second block was varied by substituting in a lysine for the purpose of cross-linking. The third block was the human fibronectin domain with a cell attachment sequence, REDV. A final sequence of VGVAPG, was inserted as an elastase target sequence for processability. The entire monomer is shown in figure 2.1.

[(**VPGIG**)$_2$ – (VPGKG) – (**VPGIG**)$_2$ – (EEIQIGHIPREDVDYHLYP) - (**VPGIG**)$_2$- (VPGKG) – (**VPGIG**)$_2$ – (**VGVAPG**)]

Figure 2.1. – ELP monomer sequence designed to mimic the extracellular matrix

Lim et al. demonstrated the ability to rapidly cross-link ELP hydrogels in aqueous solutions by the addition of an organophosphorous cross-linker, THPP acid, under physiological conditions [35]. The overall objective was to create *in situ* gelation of injectable ELPs for minimally invasive implantation of biomaterials and tissue engineering scaffolds. The ELPs were designed to have a sequence of KV7F-9. The authors showed that the mechanical properties of the THPP-cross linked ELPs were modulated by the concentration of the lysine residues and by the pH of the reaction. The authors also showed that fibroblasts were able to be encapsulated in the ELPs and were able to survive the cross-linking procedure for 3 days.

The same group cross-linked ELP block copolymers with hydroxymehylphosphines (HMP's) in aqueous solution [36]. The ELPs were composed of two different groups A and B, with cross-linkable with lysine residues and hydrophobic blocks with no cross linking sites were synthesized and the effects of the residues in each block were examined. All of the blocks were rapidly cross-linked in several minutes under physiological conditions. The survival rate of fibroblasts was again found to be 3 days in vitro. The cells were seen to be more viable within the tri-block hydrogels than in the mono-block gels at the end of day 3. This study showed that the mechanical properties of ELP hydrogels and the environment that they provide for cells were able to be tuned by the design of the block copolymers.

2.3 ELPs Used as Switching Mechanisms

ELPs nanostructures were grafted onto thiolates patterned onto gold surfaces by dip-pen nanolithography by Hyun et. al [37]. The biomolecular switch designed by the authors contained two components. The first was a stimuli-responsive ELP grafted onto the gold surface and the second was an ELP fusion protein. The two components were able to be reversibly associated and dissociated on a surface by initiating phase transition behavior of the surface bound ELP and of the fusion protein in solution. This result demonstrated the possibility of ELPs to be reversible switches for capture and release of a small number of proteins integrated into nanoscale devices.

Microcantilever sensing and actuation abilities of end-grafted ELPs were investigated by Valiaev [38]. The ELP sequence was varied to include different variations of lysine, valine and phenylalanine. Phase transitional behavior of ELPs led to

considerable changes in the surface stresses in the ELP graft layer as well as detectable changes in microcantilever deflection. The LCST behavior was triggered by changes in solution pH and ionic strength. Atomic force microscopy (AFM) was used to detect microcantilever deflection and quartz microbalance measurements (QCM) was used to detect the mechanical changes of ELPs. The authors demonstrate the potential for ELPs to be used for cantilever actuation and sensing applications in microfluidic devices. Single force spectroscopy studies [39] showed that the molecular elongation resulted from force induced prolyl-cis trans isomerization in proline residues, which are present in all ELPs. Hugel and Urry investigated the single-force extension curves for poly(GVGVP) and poly(GVGIP) in order to distinguish the mechanism of elasticity in ELPs [40].

2.4 ELPs used as Drug-Delivery Systems

The responsive behavior of ELPs makes them ideal for use in drug delivery systems. Two important factors affecting the ability of polymeric drug delivery are pharmokinetics and biodistribution are controlled by the molecular weight and amino acid sequence of the polymer [41]. ELPs have the ability to precisely control these two parameters. The tunable nature of the transition temperature or ELPs allows them to be tuned to physiologic temperatures. Finally, since ELPs are composed of amino acids they are biodegradable in the body.

Chilkoti [42] synthesized two ELPs of different compositions with one having a higher T_t than the other due to higher hydrophilic character. ELP1 had T_t's that were approximately 37 °C as well as a molecular weight of 59.5 kDa. ELP2 had a T_t that was approximately 52°C with a molecular weight of 61 kDa. The ELPs were injected into

nude mice which contained human tumor xenographs and observed by intravital microscopy. This imaging technique showed that ELP1 aggregated within the blood of tumors that were heated. ELP2 did not aggregate under these conditions. This was the first study to demonstrate that an ELP would undergo phase transition inside a tumor at a desired temperature [42].

Silk elastin like polypeptides (SELPs) are polypeptides that contain repeating motifs from both silk and elastin proteins [2]. These hybridized ELP materials with silk form injectable hydrogels that function as a depot for localized delivery of drugs [41]. Capello increased the solubility and responsiveness of an SELP by including the ELP repeat unit VPGVG [43]. This SELP maintained the crystallinity of silk but it showed increased flexibility because of the ELPs. Nagreskar et al. added hydrophobic character to a hydrophilic SELP and demonstrated the ability to lower the transition temperature [44]. They also demonstrated that the SELPs were sensitive to pH and ionic strength changes. Other researchers have shown that the ability to adjust SELPs using these parameters makes them viable for gene delivery systems [45,46].

2.5 Plasmid DNA

Bacterial plasmid DNA are closed circular molecules of double stranded DNA that range in size from 1-200 kb [47]. They are capable of autonomous replication in a cell and are commonly used as cloning vectors. Plasmids contain genes that code for enzymes that can be used in advantageous ways by the host cells. The most commonly used plasmids in recombinant DNA techniques are able to replicate in Escherichia *coli* (*E. coli*). In order to simplify their usage, most manufacturers shorten the length to < 4 kb.

For instance the pUC19 cloning vector used in this study is of a length of 2786 base pairs and the pET20b expression vector is 3712 base pairs. Plasmid vectors typically contain nothing more than essential nucleotide sequences for use in DNA cloning, which are a replication origin, a drug resistant gene and a region where DNA fragments can be inserted. This is represented in figure 2.2.

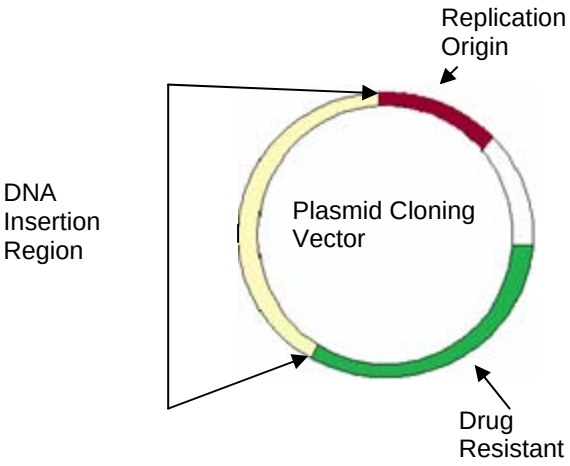

Figure 2.2 Typical plasmid cloning vector

The replication origin is a specific DNA sequence of 50-100 base pairs present in plasmids which enables them to replicate. Host cells enzymes bind to this replication origin which initiates replication of the plasmid and once it is initiated replication continues along the circular plasmid. Therefore any DNA sequence inserted into the plasmid is replicated along with the rest of the plasmid DNA.

The term transformation is used to describe the genetic alteration of a cell caused by the insertion of foreign DNA. This ability allows plasmids vectors to be introduced and expressed by *E. coli* cells. The drug resistant region in a plasmid encodes an enzyme that inactivates a specific antibiotic. After plasmid vectors are put into *E. coli*, the cells that take up the plasmid can be easily selected from the larger number of cells that do not by growing them in a medium that contains ampicilin. Normally *E. coli* cells can not take

up plasmid DNA from the medium, but exposure to the $CaCl_2$ present in competent cells allows them to take up the foreign DNA. Each competent cell incorporates a single plasmid DNA molecule, which contains the drug resistant gene. When placed on agar plates containing the antibiotic, only the transformed cells containing the drug resistant gene will survive. A DNA fragment can be inserted into the plasmid vector and when this construct transforms an *E. coli* cell the cells that are produced will contain the same inserted sequence of DNA. The inserted DNA is replicated along with the rest of the plasmid DNA and segregates to daughter cells as the colony grows. This process allows the initial fragment of inserted DNA to be replicated in the colony of cells into a large number of identical copies. All of the cells in a colony arise from a single transformed cell and thus they are considered cloned cells. The initial fragment of DNA inserted into the plasmid is referred to as cloned DNA [47].

2.6 Restriction Enzymes

Restriction enzymes recognize specific sequences of base pairs, typically 4 to 8 base pairs in length, called restriction sites. They then cleave both strands of DNA at this site. Restriction sites are inverted and thus the sequence is the same on each strand of DNA when read in the 5' to 3' direction. The restriction enzymes cut the DNA into a set of reproducible fragments called restriction fragments. A restriction enzyme also restricts incoming foreign DNA by cleaving it at all of the restriction sites in the DNA.

Restriction enzymes make staggered cuts in the two DNA strands as shown in figure 2.3. This generates fragments that have single stranded tails at both ends. Tails generated at restriction sites are complementary to those on all other fragments generated

by similar restriction enzymes. These single stranded regions are called “sticky ends” [47] and are capable of transiently base pairing with those on the other DNA fragments within the same restriction enzyme site. The process of base pairing sticky ends of DNA allows differing DNA to be ligated.

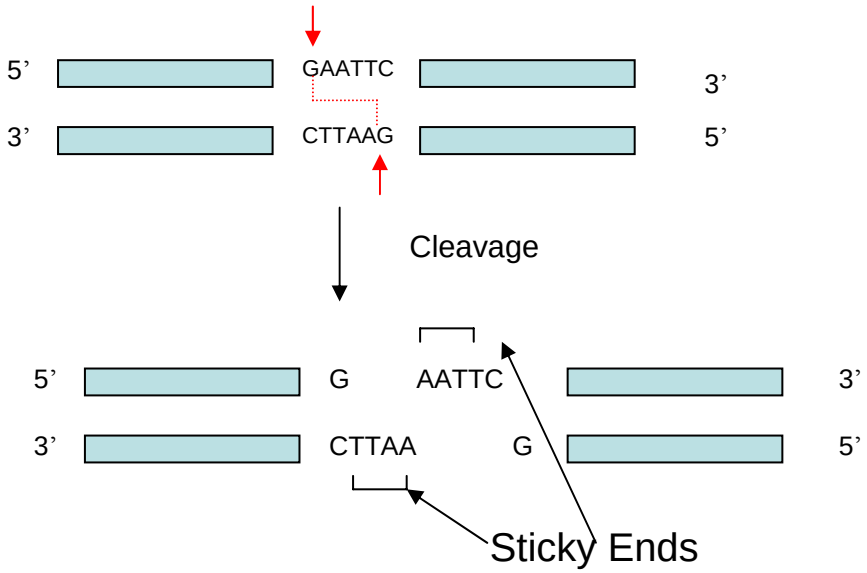

Figure 2.3 Restriction enzyme digestion producing sticky ends

DNA ligase covalently links restriction fragments in vitro. This purified enzyme catalyzes the formation of 3’ to 5’ phospho-diester bond between the 3’ hydroxyl end of one restriction enzyme fragment and the 5’ phosphate end of the other fragment during base pairing. Therefore when DNA ligase supplemented with ATP is added to a mixture containing restriction fragments with sticky ends, the restriction fragments are covalently ligated together.

2.7 Recursive Directional Ligation

A strategy was developed by Meyer and Chilkoti [48] which synthesized genes encoding repetitive protein based polymers composed of a specific amino acid sequence, chain length and composition. The method was termed recursive directional ligation (RDL) [48] and is schematically represented in figure 2.4. The basic concept behind this method is the integration of short gene segments using recombinant DNA techniques. Beginning with a monomer, this controlled stepwise oligomerization can produce a library of oligomers spanning a desired chain length. This method has an advantage over traditional methods of polymerization by offering precise control and rapid controllable results.

Different strategies have been developed to assemble synthetic genes for repetitive polypeptides. Concatemerization is a process that is capable of synthesizing a complete library of oligomeric genes. A library synthesized using this method will produce genes that encode oligomers with the same DNA sequence but of different sizes. This process however, offers the user no control, because it is a statistical process that yields a population of DNA oligomers with a distribution of different lengths and molecular weights. Therefore there is no way to guarantee a specified length of a gene although the sequence is guaranteed.

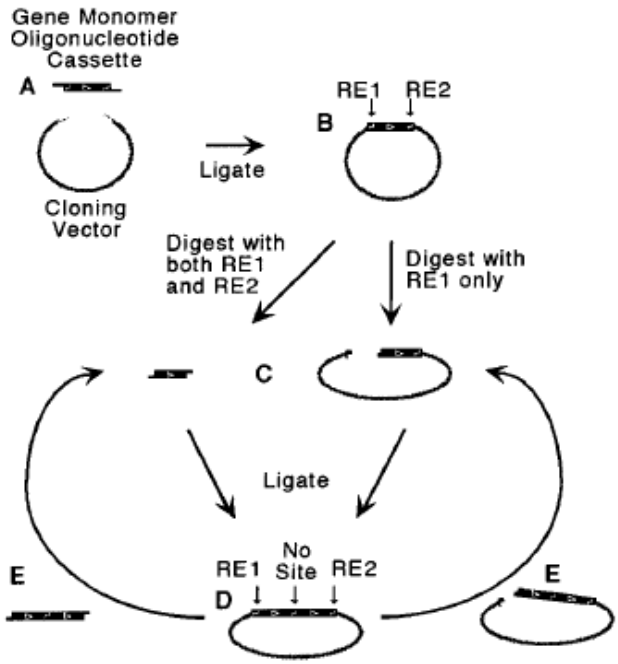

Figure 2.4 Overview of RDL schematic

A synthetic oligonucleotide cassette containing the monomer gene is annealed using PCR and ligated into a cloning vector such as pUC19. Oligonucleotides in this case were designed so that EcoRI and HinDIII compatible cohesive ends are created after annealing, which allow the annealed product to be directly ligated into the EcoRI and HinDIII cleaved pUC19. The design of the monomer gene is designed to encode a defined number of pentapeptide repeats, while incorporating two additional restriction enzyme recognition sites on each end of the coding sequence internal to the already present EcoRI and HinDIII sites. These additional sites are labeled RE1 and RE2 and are used to oligomerize the gene by the following method.

- An insert is produced by digesting the plasmid that contains the monomer gene with both RE1 and RE2

- The cloning vector is linearized vector produced by the digesting same plasmid with only RE1
- Purified insert is ligated into the linearized vector which results in dimerization of the gene

The monomer gene is designed so that RDL achieves three goals:

1) Insert is ligated with its directionality preserved in a head-to tail orientation upon ligation into the vector
2) The ligation does not introduce extra residues at the ligation site
3) The original recognition sites for RE1 and RE2 are maintained at each end of the dimerized gene, but neither recognition site is generated at the internal site of ligation

The end result of this method is that the oligomer synthesized in any round of RDL can be used in subsequent rounds of RDL as either the insert or the vector.

Selection of RE1 and RE2 for RDL

The selection of the restriction enzymes must satisfy four important requirements:

1) Must have different recognition sequences so that the DNA can be selectively cleaved by either one and that neither site is re-formed at the internal site of ligation
2) The two must produce complimentary, single stranded DNA overhangs upon cleavage
3) At least one of the two sites should be unique on the cloning vector so that digestion with the enzyme cleaves the plasmid only at the single site

4) Recognition sequence of both RE's must be compatible with the coding sequence so that when the two are ligated together, the repeat sequence of the ELP is not disrupted at the internal ligation site

The authors chose the restriction endonuclease pair PflMI and BglI for the following reasons. The pair has different recognition sequences, meeting requirement 1. They also produce overhangs upon cleavage. This is useful for two reasons. The first of which is that it allows for the selection of the same overhang sequence for both enzymes which was 5'GGC-3'. This means that the ends created by a digestion with PflMI are compatible with those created by digestion with BglI, which meets the second requirement. Since the resulting overhang bases are non-palindromic, it means that the ligation must proceed in a head-to-tail fashion.

The puc19 cloning vector has no PflMI restriction sites native, so its addition meets the third requirement outlined above. This allows the vector to be linearized to accept the insert. BglI has two recognition sites in Puc19 which means that when a double digestion is performed with PflMI and BglI four gene fragments are produced. These can be separated by agarose gel electrophoresis which allows for selection of the appropriate band. The restriction enzymes chosen must be compatible with the gene sequence. There must be recognition sites for RE1 and 2 at opposite ends of the gene and the repetitive sequence must not be disturbed when a fragment digested with RE1 is ligated into a RE2 cleaved end.

2.8 Oligomerization Domains: Foldon

Fibritin is a structural protein of bacteriophage T4, which belongs to a class of chaperones that catalyze specific phage-assembly processes [49]. T4 fibritin is a three stranded segmented α-helical coiled-coil protein that contains a small trimeric globular domain located at its C terminus [49,50,51,52,53], shown in figure 2.5. This globular, C-terminal domain has been termed foldon [51,52,53]. Oligomerization domains can be used for many purposes. In natural or obligatory trimers, the proteins will form a native or defined fold in an oligomeric state due to the presence of the oligomerization domain. The domains associate with extremely fast kinetics and increase the stability of the other domains in the protein. Oligomerization leads to functional advantages including multivalency and high binding strength, increased stabilization and the ability to combine the functionality of multiple domains. Thus using protein engineering techniques oligomerization domains can be attached to the functional domains of many proteins and the resulting changes in their properties can be investigated [50].

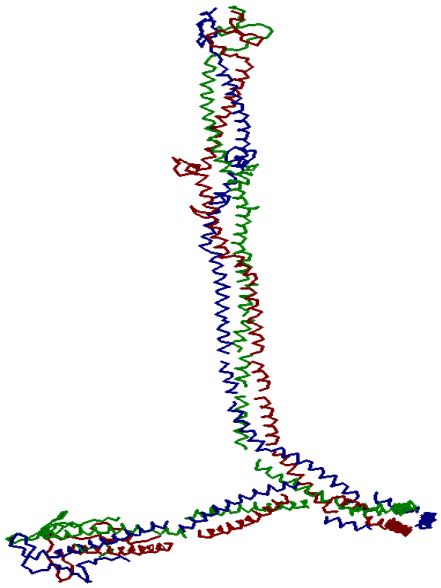

Figure 2.5: T4 Fibritin. Three stranded coiled-coil with foldon domain. Image modeled in Swiss PDB viewer.

2.9 Structure and Use of Foldon

Tao et. al determined the structure of the foldon domain at the molecular level to a resolution of 2.2 A by X-ray crystallography. The results showed that in T4 fibritin there is a domain composed of three identical subunits of 119 amino acids as well as a small globular trimeric domain at the C terminus. The three subunits of fibritin associate into a trimer, which forms a parallel α-helical coiled-coil along the crystallographic axis. Each α-helix is separated by insertion loops and hydrogen bonds are formed between consecutive helical segments which allow the subunits to form continuous coiled coil.

The small globular domain located at the C terminal in T4 fibritin there is termed foldon [51,52] and is shown in figure 2.6. This domain consists of 30 residues from each subunit. Each subunit contains a C terminal region that has a β-hairpin motif and a loop connecting the β-hairpin to the end of the last α-helical segment [49]. Within the subunit the connecting loop is stabilized by hydrophobic interactions and hydrogen bonds. Specifically, residues Tyr458, Ile459, Trp476, Val470, Leu479, Phe482 and Leu483 form a hydrophobic interior within the C-terminal of the trimer. The 3 related β-hairpins are stabilized by five main chain hydrogen bonds. This domain eventually forms a β-propeller like structure with a hydrophobic interior [49, 52].

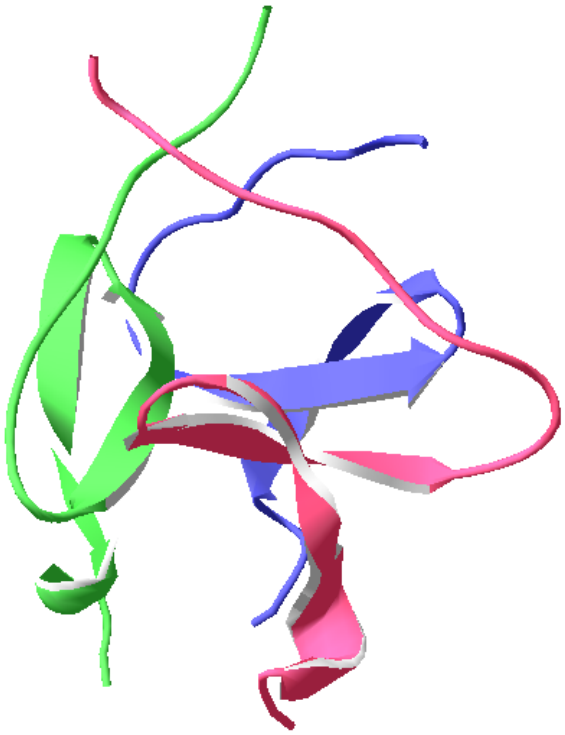

Figure 2.6. C terminal domain of fibritin T4, termed foldon. Image produced using Swiss-Pdb Viewer Software Program

The trimerizing mechanism [55] was investigated by expressing a number of truncated fibritin molecules in *E. coli*. All of the mutants formed soluble expression products except for the mutants that did not have the residues which formed the hydrophobic interior of the C-terminal domain. This led to the conclusion that the hydrophobic residues were essential for trimerization in T4 fibritin. The function of the foldon domain is then the correct alignment and registration of three subunits. Polypeptides containing the complete foldon domain will then be able to form trimers.

The foldon domain was used as a stabilizing trimer in collagen triple helices by Frank [51] and Du [53]. By fusing collagen like peptides to the N terminus of the foldon domain, Frank et al. were able to improve the thermal stability of $(GPP)_{10}$, by showing

the mid-point temperature of triple helix unfolding was significantly increased. This structure is shown in figure 2.7.

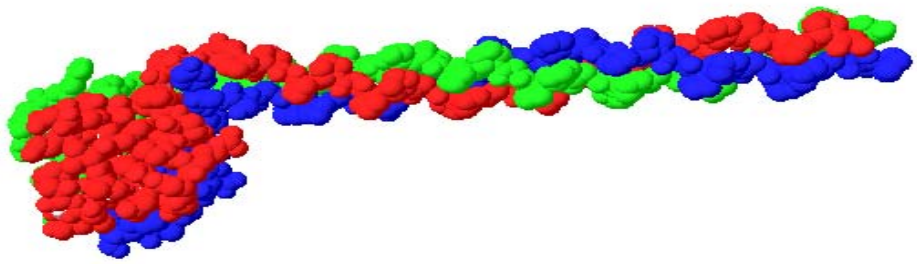

Figure 2.7. Collage $(GPP)_{10}$ repeats with attached foldon domain. Image modeled using Swiss PDB viewer program.

The addition of the foldon domain also rendered triple helix formation concentration independent. This concentration independence also increased stabilization of the triple helix and an increase in the folding rate. The stabilization is thought to be a function of the high local concentration in of the foldon domain due to the close vicinity of its N termini for the C termini of collagen like peptides. Circular dichroism confirmed that foldon formed a β structure at 215 nm which was consistent with the findings of Tao [49] and indicated that the protein folded correctly. Analytical ultracentrifugation showed molecular mass of 9.8 kDa for the foldon compared to 3.2 kDa for the monomer, indicating trimer formation. Du et al. [53] fused to the C-terminal of collagen like peptides and the thermal stability was assessed. Differential scanning calorimetry and thermogravimetric analysis were used and the results showed that collagens with the

attached foldon sequence had a 7 °C higher thermal denaturation temperature. SDS-page analysis confirmed trimer formation of the proteins. Triple helix formation was confirmed by an FT-IR comparison of the monomer and the monomer plus foldon.

The crystal structure of collagen GPP_{10}-foldon was determined by Frank in 2003 [52]. Analysis at 2.6 Å resolution revealed conformational changes within the interface of both domains as compared to the structure of the individual molecules. Trimerization leads to a high local concentration of collagen chains, which leads to triple helix nucleation by entropic reasons [52] and the foldon domain itself forms a trimeric nucleus which is necessary of the formation of a triple stranded coiled coil. The interface between the $(GPP)_{10}$ and the foldon domain was analyzed and the new construct was compared with the structure of the individual molecules. Within the crystal lattice of $(GPP)_{10}$ the foldon domains were seen to be arranged in a distinctly ordered manner and thought to be interacting via electrostatic interactions and substantially stabilized by these interactions. The foldon subunits were determined to be oriented in a manner that resulted in a three dimensional assembly which resulted in the subunits having a tail to tail type arrangement. The interface between the $(GPP)_{10}$ and the foldon domain was found to be stabilized by a pattern of hydrogen bonds and the three chains were found to have hydrogen bonds between themselves and the foldon domain at different residues, but the chains themselves did not have hydrogen bonds between themselves [52].

We will be attaching the foldon domain to the C-terminal of our synthesized ELP constructs. We theorize that this will improve the thermal stability of the constructs, improve folding kinetics and increase the intrinsic concentration of the ELPs. The foldon domain will help ELP triple strands find each other by being attached to the three

subunits of the foldon domain. The close proximity and increased hydrophobic character as well as increased concentration will increase the efficiency of chain folding and aggregation. Molecular models of ELPs containing the attached foldon domain at temperatures above and below the transition temperature are shown in figures 2.8 and 2.9.

Figure 2.8: (GVGVP)n-foldon shown as three ELP chains connected to the foldon domain in the unfolded state below the transition temperature. Image modeled in Swiss PDB viewer

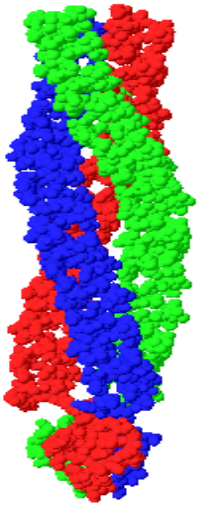

Figure 2.9: (GVGVP)n-foldon as three ELP triple strands in the folded state above the transition temperature. Image modeled in Swiss PDB viewer program

2.10 Methods to Vary the Transition Temperature of ELPs

This section details the numerous methods described in literature that are used to alter the T_t of ELPs. These methods include, ELP concentration, ELP chain length and solution parameters such as NaCl concentration.

2.11 NaCl Concentration as a Method to Lower the T_t of ELPs

Numerous groups have investigated the addition of NaCl as a means to lower the T_t of ELP's. Urry, Cabello et al. investigagted the effect of NaCl on the exothermic and endothermic components of the LCST [56] by making use of temperature modulated differential scanning calorimetry (TMDSC), a technique that is able to separate the two components [57]. NaCl causes a significant and concentration dependent decrease in the LCST [56] as well as an increase in the transition enthalpy (ΔH_t). Typical DSC thermograms show an decrease in the T_t with increasing NaCl concentration and the area under the endotherm is taken as the enthalpy. According to Urry and Cabello [56, 57] the endothermic peak of a DSC can be described as an increase in the order of the system by increasing the waters of hydrophobic hydration. Exothermic behavior is described as the folding and association while the endothermic behavior is the disruption of ordered water structures. Both of these components increase with the addition of NaCl. The total effect is explained as an increase in the hydrophobicity of the chain, which causes a decrease in T_t and an increase in the enthalpy. The authors conclude that the effect of NaCl is to cause increased organization of ELPs in the folded state and an improved structure of hydrophobic hydration surrounding the chain [57].

Nuhn and Klok [58] investigated the secondary structure formation and T_t behavior of short ELPs in 2008. This study focused on the T_t behavior of ELPs ranging in length from 1 to 6 pentapeptide repeats. Other studies have focused on this behavior [59, 60, 61] but have not focused on multiple factors effecting T_t. For very short ELPs the T_t may not be measurable in UV-vis spectrophotometers due to the temperature control limits. Typical UV-vis spectrophotometers are able to operate in a temperature range between 10 – 100 °C. To overcome these equipment limitations the authors added NaCl in various concentrations to the ELP and extrapolated to zero NaCl concentration to find the reported T_t value [58]. Protein solutions were measured at 10 mg / ml. The authors report the T_t of $(GVGVP)_5$ to be 124° C at 0 M NaCl and report an T_t of 40°C at 3 M NaCl concentration. This large difference is much higher than that reported for ELPs of higher molecular weight [62]. In a study based on higher molecular weight ELPs, Urry et al. reported a linear dependent decrease of T_t on NaCl concentration, but the reported difference was 14 °C / per repeat unit [62]. The authors concluded from this that the T_t's of short ELPs are more sensitive to the addition of NaCl than longer chains.

Yamoka et al. investigated the effects of the addition of NaCl and other additives such as SDS on the T_t of $(VPGIG)_{40}$ [63]. With the addition of increasing NaCl, KCl and $K2SO_4$ concentrations there was a linear decrease in T_t. Interestingly $K2SO_4$ drops the T_t more sharply than the other salts, which the authors were not able to explain. The addition of SDS at different concentrations was shown to have a strong effect on the LCST behavior. Adding SDS at values higher than the critical micelle constant of SDS [64] caused the disappearance of T_t, while values of SDS lower than CMC caused a gradual increase in T_t. The authors explained these effects in the following way. Salts,

such as NaCl that have a lower lyotropic numbers induce the globular state of polymers [65]. These salts act in a manner that strengthens the hydyophobic interactions which allow ELPs to hydrophobically fold and assemble and thus lower the LCST [63].

2.12. Effect of ELP Concentration and Chain Length on T_t

The effects of peptide concentration on the LCST behavior of ELPs has been extensively studied and shown to have strong effects. Urry described the phase diagram related to ELPs [66] and showed that in the two-phase region there is strong concentration dependence. In other words, at low ELP concentrations there is a dramatic increase in T_t. This concept was also supported by the work of Meyer and Chilkoti in 2004 [67]. They described multivariate equations that described the T_t as functions of chain length, concentration and specific constants. The results from this study showed that ELP concentration and chain length have a greater impact on ELPs that are of low peptide concentration and of small chain length. It has been well documented that ELPs of shorter chain length have higher T_t values than larger chain lengths [58, 67]. Urry [68] described the effects of ELP concentration in two ways. The first effect was that at low ELP concentrations the T_t increased because the interchain cooperativity needed for ELPs to fold correctly does not take place as efficiently in dilute peptide conditions. The study showed that there existed a concentration limit where the effect of increasing the ELP concentration no longer had an effect on the T_t [68]. The second effect of ELP concentration was that at extremely high concentrations there was an inability for the ELP to go from the unfolded state to the completely hydrated folded state [68]. This situation also causes an increase in T_t.

The effects of molecular weight were studied by Cabello and Reguera in 2004 [34]. The authors showed that the T_t decreased as the molecular weight increased. This also corresponded with an increase in the transition enthalpy. The most striking effects took place as low molecular weights were increased (e.g from 10,000 to 20,000 Da) but as the molecular weight kept increasing the effects reached asymptotic levels. The overall effect of increasing the molecular weight was seen to be similar to the changes seen in changing the mean polarity of the ELPs such that lowering the molecular weight is similar to decreasing the mean hydrophobicity of the ELP.

CHAPTER III

MATERIALS AND METHODS

3.1 Overview

This section details the methods and materials used to construct, prepare and characterize the proteins used in this study. There are two main groups of constructs that were developed based on the poly(GVGVP) motifs which are essentially similar. The first class of ELPs are GVGVP polymers ranging from $(GVGVP)_{10}$ to $(GVGVP)_{60}$. The second class of ELPs involve the addition of an oligomerization domain, termed foldon, to the C terminal of GVGVP which range from $(GVGVP)_{10}$-foldon to $(GVGVP)_{60}$-foldon.

3.2 Synthesis and Cloning of the ELPs

The synthesis and construction of the GVGVP molecules is based on the method laid out by Chilkoti and Meyer in 2002 [48]. The addition of the foldon domain was inspired by the work of Frank and Kammerer [51].

The host strain for all gene cloning and synthesis was *E.coli* strain BL21 star (Invitrogen inc.). The cloning vector was pUC19 and pET20b was used as the expression vector (both from Novagen Inc.). We started with custom made oligonucleotides (Invitrogen Inc.) that encoded 5 repeats of the GVGVP peptide, which were termed MC5 forward and reverse. The amino acid sequence is as follows:

GVGVP Forward MC 5 Oligonucleotide

5' to 3'

AATTCATATGGGCCACGGCGTGGGTGTTCCGGGCGTAGGTGTCCCAGGTGTGGGCGTAC
CGGGCGTTGGTGTTCCTGGT

GVGVP REVERSE MC 5 Oligonucleotide

3' to 5'

AGCTTGCCAGCCCGGCACGCCGACACCAGGAACACCAACGCCCGGTACGCCCACACCTG
GGACACCTACGCCCGGAA

Reverse HindIII Primer

5' to 3'

GGTCAAGCTTGGATCCGAAGAC

Forward EcoRI Primer

5' to 3'

GCCAGAATTCGCAGCATACATATGG

The annealing of forward and reverse MC5 was performed in a thermo-cycler (Thermo Electron Corp.) utilizing a polymerase chain reaction (PCR). The reactions contained 1 µl of template primers, 10 µl forward EcoRI primer, 10 µl reverse HindIII primer, nuclease free water and 1 x PCR master mix (both from Promega Corp.) to a total reaction volume of 100 µl. The reaction was heated to 95°C for 5 minutes and then cooled down to room temperature at a rate of 1.5 °C / min for 70 cycles. Then the mixture was held at 4 °C for 55 minutes. The resulting sequence represents an annealed double stranded GVGVP$_5$ mer DNA cassette with EcoRI and HindIII compatible ends.

The final sequence for double stranded DNA for GVGVP-5mer is:

```
EcoRI                                PflmI
A ATT CAT ATG GGC CAC GGC GTG GGT GTT CCG GGC GTA GGT GTC
                          V   G   V   P   G   V   G   V

CCA GGT GTG GGC GTA CCG GGC GTT GGT GTT CCT GGT GTC GGC GTG
 P   G   V   G   V   P   G   V   G   V   P   G   V   G   V
        BglI   HinD III
CCG GGC TGG CA
```

Yellow highlights indicate regions that indicate restriction endonuclease cut-sites. After the PCR reaction was finished the amplified DNA was run on a 2% agaorose gel in 1 x TAE buffer (40 mM Tris acetate, 2 mM EDTA, pH 8.5) at 80 V. The sample was mixed with 6x load dye (Promega Corp.) to a total volume of 120 µl. 100 base pair DNA ladder was run next to the sample in order to select the appropriate band for excising. The sample length is 98 base pairs and therefore we excised a band at 100 base pair on the agarose gel. The gel slice was weighed and purified using a DNA gel extraction kit (Genscript Corp.) and eluted in double distilled water.

Annealed GVGVP was ligated into a pUC19 cloning vector that was doubly digested with HinDIII and EcoRI. The procedure for the double digestion is as follows.

Component	Amount
- Puc19 DNA	3 µl
- EcoRI Restriction Enzyme	1 µl
- NdEI Restriction Enzyme	1 µl
- 10 x buffer (EcoRI Buffer)	1.5 µl
- Nuclease Free Water	8.5 µl

The above components were combined in a 1.5 ml microcentrifuge tube. Restriction enzymes must be handled with care and should not be vortexed or kept out of the -20° C freezer for more than the time needed put them into the reaction. After the components were mixed, they were briefly centrifuged to ensure that the restriction enzymes were fully mixed into the reaction. The digestion was incubated at 37 ° C for two hours. After the reaction was completed, the product was run on a 1.5 % agaorose gel in order to determine if the digestion was successful or not.

The pUC19 vector is cut once by HinDIII at 396 base pairs and once by EcoRI at 447 base pairs. The corresponding band we were looking for at the end of the double digestion was located at 98 base pairs. The band was excised and purified by a DNA gel extraction kit (Genscript Corp.). The resulting DNA was used as the vector for subsequent ligation reactions.

The GVGVP samples were then double digested. The procedure for $(GVGVP)_5$ double digestion with EcoRI and HinDIII is as follows:

Component	Amount
- GVGVP 5mer DNA	8 µl
- EcoRI Restriction Enzyme	4 µl
- NdEI Restriction Enzyme	4 µl
- 10x buffer (EcoRI Buffer)	5 µl
- Nuclease Free Water	29 µl

The rest of the procedure is the same as previously described. The reaction product was run on an agarose gel and the appropriate band was excised.

The next step in the process was to insert the annealed and cleaved $(GVGVP)_5$ inserts into the linearized pUC19 vector. We used a quick ligation kit (New England Biolabs) to perform the ligation. The ligation kit enables the ligation of blunt ends or cohesive end DNA fragments in 5 minutes at room temperature. The components of the kit are; Quick T4 DNA ligase (50 mM KCL, 10 mM Tris-HCL (pH 7.4), 0.1 mM EDTA, 1 mM dithiothreitol and 50 % glycerol), and 2X quick Ligation Reaction Buffer (132 mM Tris-HCL, 20 mM $MgCl_2$, 2mM dithiothreitol, 2mM ATP, 15 % polyethylene glycol at a pH of 7.6). The quick ligation protocol is:

1. Combine 50 ng of vector with a 3-fold molar excess of insert. Adjust volume to 10 µl with dH_2O.
2. Add 10 µl of 2X Quick Ligation Reaction Buffer and mix.
3. Add 1 µl of Quick T4 DNA Ligase and mix thoroughly.
4. Centrifuge briefly and incubate at room temperature (25 ° C) for 5 minutes.
5. Chill on ice and transform or store at -20° C.

This ligation protocol produces 21 µl of product, 10 µl of which was used in the resulting transformation.

To perform the transformation we followed the recommended protocol given by New England Biolabs. BL 21 star competent cells (Invitrogen inc.) were taken out of the -70 ° C freezer and put on ice to thaw. The protocol for this and all subsequent transformations is as follows:

1. Thaw competent cells on ice
2. Chill approximately 10 µl of the ligation mixture in a 1.5 ml microcentrifuge tube.
3. Add 50 µl of competent cells to the DNA and mix gently by pipetting up and down.
4. Incubate on ice for 30 minutes.
5. Heat shock for 2 minutes at 37 ° C and chill on ice for 5 minutes after.
6. Add 950 µl of room temperature LB medium without ampicilin to the reaction and incubate at 37 ° C for 1 hour.
7. Spread 300 µl of the reaction mixture onto LB agar plates with ampicilin.
8. Incubate overnight at 37 ° C.

Colonies were selected from agar plates (see appendix) and placed into 5 ml of LB media cultures supplemented with ampicilin. The mixture was incubated overnight at 37 ° C and shaken at 300 RPM. The DNA from the overnight cultures was purified using a Qiagen Plasmid Mini-Prep Kit which is designed to purify up to 20 µg of plasmid DNA from overnight *E. coli* culture in LB medium. Before performing the mini-prep, glycerol frozen stocks were made of the samples for long-term storage. The procedure for making

frozen stocks is located in the appendix. After the frozen stocks were made and transferred, the plasmid mini-prep began. The procedure for this and all subsequent mini-preps is located in the appendix.

At this point we have a pUC19 vector which contains annealed $(GVGVP)_5$. In order to screen the colonies to ensure that we have the desired product we use PCR reactions. We performed two PCR reactions.

1. pUC19 vector
2. pUC19 + $(GVGVP)_5$

We used M13 forward and reverse primers (Invitrogen inc.) in the reaction, which enabled us to visualize the reaction. The procedure for the PCR is:

Component	**Amount**
- PCR Master Mix	12.5 µl
- F M13 Primer	2.5 µl
- R M13 Primer	2.5 µl
- DNA Template	1 µl
- Nuclease Free Water	6.5 µl

PCR reactions were run on the thermo cycler and the resulting product was run on 1.5 % agarose gel for screening. There should be a 50 base pair difference between the pUC19 vector and the pUC19 + $(GVGVP)_5$, which will show up as 100 and 150 base pairs on the gel respectively. At this point we have Puc19 + $(GVGVP)_5$ and are ready for subsequent rounds of recursive directional ligation.

To go from a $(GVGVP)_5$ insert to a $(GVGVP)_{10}$ insert we used PCR amplification from the $(GVGVP)_5$. 15 µl of the reaction was double digested in the following manner:

Double Digestion of $(GVGVP)_5$

Component	Amount
- GVGVP-5 DNA (PCR Amplified)	15 µl
- 10X Buffer 3	3 µl
- Bovine Serum Albumin (BSA)	0.5 µl
- PflMI Restriction Enzyme	1 µl
- BglI Restriction Enzyme	1 µl

Puc19 + $(GVGVP)_5$ samples were then single digested to be used as a linearized vector for inserting the double digested $(GVGVP)_5$. The single digestion of $(GVGVP)_5$ was performed in the following manner:

Single Digestion of $(GVGVP)_5$

Component	Amount
- GVGVP 5 DNA	10 µl
- 10 x Buffer 3	2 µl
- PflmI Restriction Enzyme	2 µl
- Nuclease Free Water	6 µl
- Bovine Serum Albumin	0.2 µl

The pUC19 cloning vector has no PflMI cut sites and therefore when the $(GVGVP)_5$ gene is inserted into the vector we introduce a PflMI cut site. PUC19 has 2 native BglI sites and a 3rd is introduced with the insertion of $(GVGVP)_5$. Therefore 4 fragments are produced when the double digestion is successful. BglI cuts pUC19-$(GVGVP)_5$ at the following locations in the vector; 251, 1018 and 2395 base pairs. PflMI cuts pUC19-

$(GVGVP)_5$ at 424 base pairs. The insert will be located at 98 base pairs for a 5 repeat insert.

The samples were run on agarose gel; the appropriate bands were excised and purified according to protocols. Single-digestion of $(GVGVP)_5$ needed to be de-phosphorylated with Antarctic Phosphatase (New England BioLabs Inc.). The purpose of this was to catalyze the removal of 5' phosphate groups from DNA. Since the de-phosphorylated fragments lack the 5' termini lack the phosphoryl termini required by ligases, the vectors are unable to self-ligate. This procedure is used to reduce the vector background noise and thus reduce the amount of failed ligations due to vector self-ligation. The single digested $(GVGVP)_5$ vector was combined with double digested $(GVGVP)_5$ insert using the ligation protocol. After PCR screening it was apparent that we had 2 samples that were $(GVGVP)_{10}$. Samples were sent to the Cleveland Clinic Genomics DNA sequencing core and were sequenced with M13 sequencing primers. After the DNA sequences were verified we continued with subsequent rounds of ligation. $(GVGVP)_{10}$ to $(GVGVP)_{40}$ proceeded in the same fashion. An example of the resulting DNA sequence (CCF Genomics Core) and amino acid composition is shown below for $(GVGVP)_{40}$.

DNA Sequence for pUC19 $(GVGVP)_{40}$

TAGTTCTCCGTGCACGTCCGACACCAGGAACACCAACGCCCGGTACGCCCACACCTGGGACACCT
ACGCCCGGAACACCCACGCCCGGCACGCCGACACCAGGAACACCAACGCCCGGTACGCCCACACC
TGGGACACCTACGCCCGGAACACCCACGCCCGGCACGCCGACACCAGGAACACCAACGCCCGGTA
CGCCCACACCTGGGACACCTACGCCCGGAACACCCACGCCCGGCACGCCGACACCAGGAACACCA
ACGCCCGGTACGCCCACACCTGGGACACCTACGCCCGGAACACCCACGCCCGGCACGCCGACACC
AGGAACACCAACGCCCGGTACGCCCACACCTGGGACACCTACGCCCGGAACACCCACGCCCGGCA
CGCCGACACCAGGAACACCAACGCCCGGTACGCCCACACCTGGGACACCTACGCCCGGAACACCC
ACGCCCGGCACGCCGACACCAGGAACACCAACGCCCGGTACGCCCACACCTGGGACACCTACGCC
CGGAACATCCACGCCCGGCACGCCGACACTAGGAACACCAACGCCCGGTACGCCCATACCTGGGA
CACCTACGCCCGGAACACCCACGTCGTGGCCCATATGAATTCGCTGGCCGTCGTTTTACAACGTC
ATGACTGGGAAAACTCTGGCGTTACCCAACTTAATCTGCTTGCAGAATATCTCCCTTTCTCCATC
TGGCGTAATAGCGAATAGGCCTGCACCGATCGCCCTTCCAACAGTTGCGCATCCTGAATGGCAAA

```
TTGCCCTTGATGCGGTATTTTTTCCTTATCATCTTGTGCGGTATTTTACATTGCATTTGGGGCAT
TCTCAGTACACTCTTGCTCTGATGCGGATATTTAAGCCAGTCCCTACCCCCGTCAATTCCGCTGA
CGCGGCCTGATGGCTTGTGTGTTCCAGCATCCCTTACAGACAAGCTGTGGCGTTTCCGGTAGCTG
CTTGTGTCTAAGTTTTCTCGTCTTTACTAAAATCAGAAAGAAAGGGCCTCTTGATAGGCTATTTT
TATAGGTTATTGTTTGGTAATAATGCTTCTTAAAGTTAAGAGCCCTTTTCGTGGAATGTGCGCCG
AACCCCATATGTTTTTTTCTCATACTTCATACATTATCCCCCCAGGAAAATATCATTTGAATGTT
TTAGTATATGTAATGGAGAGTATGTTTACGACATTTCGGGTCGCCTCATGTCTTTTTGCCGGTCT
TTGTTCCTGTTGTGGTCCCCCGTACCTTCTTGGAGACACATTCTCGAGGTCTTC
```

Translated Sequence to Protein for pUC19- $(GVGVP)_{40}$

```
MGHDVGVPGVGVPGMGVPGVGVPSVGVPGVGVPGVGVPGVGVPGVGVPGVGVPGVGVPGV   60
GVPGVGVPGVGVPGVGVPGVGVPGVGVPGVGVPGVGVPGVGVPGVGVPGVGVPGVGVPGV  120
GVPGVGVPGVGVPGVGVPGVGVPGVGVPGVGVPGVGVPGVGVPGVGVPGVGVPGVGVPGV  180
GVPGVGVPGVGVPGVGVPGVGRARRT  206
```

Expression Vector Construction

A pET20b expression vectors were purchased from Novagen Inc. and was modified to be compatible with the poly(GVGVP) genes. A SfiI endonuclease recognition site was created between the native NdEI to EcoRI sites and inserted into the pET20b vector. The purpose of this was that each time we wanted to transfer the $(GVGVP)_n$ gene from a cloning vector to an expression vector we would only have to single digest the pET20b vector with SfiI endonuclease. Primers were ordered from Invitrogen and were annealed in the manner previously described.

Forward SfiI

```
TATGAGCAAAGGGCCGGGCTGGCCGTGAT
```

Reverse SfiI

```
AATTATCACGGCCAGCCCGGCCCTTTGCTCA
```

FINAL SEQUENCE for pET20b-SfiI

SfiI

```
CAT ATG AGC AAA GGG CCG GGC TGG CCG TGA TAA TTC
GTA TAC TCG TTT CCC GGC CCG ACC GGC ACT ATT AAG
```

NdeI site **EcoRI site**

The process of transferring the $(GVGVP)_n$ genes to the expression vector was similar to the other digestion processes discussed previously. Originally the pET20b vector was singly digested with the SfiI endonuclease, as the protocols in Meyer and Chilkoti laid out [10]. When this was done the result was a poly(GVGVP) in an expression vector in the following form:

- K – $(GVGVP)_n$

We decided that the charge that was carried on the lysine (K) could cause potential problems, so we investigated ways to remove the lysine. By double digesting the pET20b vector with both SfiI and NdEI we were able to remove the lysine and replace it with a histidine (H), thus giving us the desired form:

- H – $(GVGVP)_n$

The procedure for doubly digesting the pET20b vector is:

Double Digestion of pET20b with NdEI and SfiI:

Component	**Amount**
- pET20b DNA	15 µl
- NEB 10X Buffer 4	3 µl
- NdEI restriction enzyme	1 µl
- Bovine Serum Albumin	0.4 µl
- Nuclease Free Water	14.6 µl

Combine the following components in a 500 ml tube and incubate at 37°C for 3 hours. Add 1 µl SfiI and place in 50 °C dry bath incubator (Fisher Scientific) for 2 hours. When the digestion was complete, the product was run on a 1.5 % agarose gel and the appropriate band was excised. The result of that there will be one band visible between the two cut sites located at 3435 base pairs. This band was excised and purified with a DNA gel extraction kit. The expression vector was now ready to receive the doubly digested insert. $(GVGVP)_n$ samples were then doubly digested with NdEI and BglI restriction enzymes to be inserted into the expression vector. The procedure for this was:

Double Digestion of pUC19 + $(GVGVP)_n$ with NdEI and BglI:

Component	**Amount**
- pUC19 $(GVGVP)_n$ DNA	20 µl
- NEB 10X Buffer 3	4 µl
- NdEI restriction enzyme	1.5 µl
- BglI restriction enzyme	1.5 µl
- Nuclease Free Water	13 µl

The two restriction enzymes cut the pUC19 vector in 3 places. They are

- 146 base pairs + size of the insert
- 1483 base pairs
- 2341 base pairs

Fragments are at ~750 bp, ~1500 bp and ~ 2500 bp. The sample was run next to a 1 kilo-base pair ladder on 1.5 % agarose gel. The two products were then ligated according to the previous protocol and transformed. PCR screening and DNA sequence results showed the we did in fact have H-$(GVGVP)_{10}$. The result is shown in the following sequence:

Resulting Protein Translated from the Sequence

MGHGVGVPGVGVPGVGVPGVGVPGVGVPGVGVPGVGVPGVGVPGVGVPGVGVPGWP

The green highlight indicates the histidine at the beginning of the sequence. This same process was used to obtain all H-$(GVGVP)_n$ samples.

Foldon Preparation and Plasmid Construction

Foldon [51,52], was produced by annealing two custom primers (Invitrogen) that were designed to form a foldon domain and have a SfiI recognition site.

AMINO ACID SEQUENCE FOR FOLDON

(GS)GYIPEAPRDGQAYVRKDGEWVLLSTFL

FOLDON FORWARD PRIMER

TGGCCGGGTTACATCCCGGAAGCTCCGCGTGACGGTCAGGCTTACGTTCGTAAAGA

CGGTGAATGGGTTCTGCTGTCTACCTTCCTGTGATAAGGC

FOLDON REVERSE PRIMER

CGGTGAATGGGTTCTGCTGTCTACCTTCCTGTGATAAGGC

GCCACTTACCCAAGACGACAGATGGAAGGACACTATT

Yellow highlights indicate SfiI cut sites. The two foldon primers were annealed using the same procedure as described before. The annealed foldon primers were then directly ligated into a pET20b vector that was single digested with SfiI endonuclease.

pET20b vector with foldon domain is:

NdeI SfiI
CATATGAGCAAAGGGCCGGGCTGGCCGGGTTACATCCCGGAAGCTCCGCGTGACGGTCA

GGCTTACGTTCGTAAAGACGGTGAATGGGTTCTGCTGTCTACCTTCCTGTGATAAGGC

The desired form of our library of ELPs with foldon was H-(GVGVP)-$_n$-foldon. In order to achieve this goal the pET20b-SfiI-foldon vector was double digested with SfiI and NdEI. The $(GVGVP)_n$ insert was double digested with NdEI and BglI in the same manner as previously described. The resulting protein translation for a sample of H-$(GVGVP)_{10}$-foldon is shown below:

Protein Translated from this Sequence H-$(GVGVP)_{10}$-foldon

MGHGVGVPGVGVPGVGVPGVGVPGVGVPGVGVPGVGVPGVGVPGVGVPGWPGYIP 60
EAPRDGQAYVRKDGEWVLLSTFL

Yellow highlights indicate the foldon on the C terminus of the protein. The green highlight indicates the histidine at the beginning of the sequence.

3.3 Expression and Purification of ELPs

To express and purify the protein we followed the inverse transition temperature cycling method laid out by Urry and colleagues [10, 48]. The ELP encoded genes were in pET20B vectors, or expression vectors. They were then transformed to *E.Coli* for expression. For growth medium we used Luria-Bertani (LB) media. To make the media we combined 5 g NaCl, 5g Yeast extract and 10 g Peptone into 1liter of pure H20 and autoclaved the flask.

Starter cultures were created by transferring transformed cells either from a fresh agar plate or from glycerol frozen stocks into 10 ml of LB media with ampicilin. The cultures were then incubated overnight (~12 hours) at 37°C with shaking at 300 RPM. The liter of LB media was supplemented with 1000x ampicilin stock solution (1ml stock into 1 L media). The starter culture was transferred to the media to begin expression. Cell density measurements were taken and when the OD_{600} reached ~0.8-1.0 [48] expression was induced by the addition of IPTG at a concentration of 1mM (240 mg into 1 L). Shaking continued for 3.5 hours at 37°C and 300 RPM. The liter was then transferred to two 500 ml centrifuge tubes and centrifuged with a Beckman J2-21 centrifuge at 3000g for 15 min at 4 C. The supernatants were discarded and the pellets were kept for purification in -20°C.

ELPs are purified by inverse transition cycling [10] which is a process of selective aggregation by heating the cell lysate and / or adding NaCl. The frozen pellets were taken out of the freezer and thawed before resuspension. 10 ml of cold BPER II (20 mM Tris-HCL pH 7.5) solution (Pierce) was mixed into each 500 ml tubes and the pellets were resuspended by vortexing. Once the pellets were completely resuspended they were centrifuged again at 10000g and 4°C. At this point the protein is in two fractions, insoluble and soluble. SDS-PAGE analysis has shown that the protein exists in the soluble fraction. The supernatant (the soluble fraction) is taken and undergoes a warm centrifugation step. First the supernatants are placed in an incubator set at a temperature that is higher than the known or expected T_t of the ELP while a water bath is prepared at a similar temperature. Warm centrifugation occurs in a separate laboratory, so we use the water bath to ensure that the ELPs do not go below their T_t at any point during the

process. Centrifugation then occurs at 16-17,000 RPM at a temperature of 40-45 °C for 15-20 minutes. When the centrifugation is complete the supernatant must be immediately decanted and discarded to ensure that none of the pellet, which contains the ELP, goes back into solution. Pellets were put onto ice and re-suspended in 5 mL of cold, low ionic strength buffer (PBS: 137 mM NaCl, 2.7 mM KCL, 4.2 mM $Na2HPO_4$, 1.4 mM $KH2PO_4$ at a pH of 7.3). The resuspended pellets were centrifuged at 10-11,000 g at 4 °C for 15 minutes. At the end of this stage there should be a small clear looking pellet and supernatant. The supernatant is transferred to another tube and the first round of inverse transition cycling is complete.

The second round begins with the supernatant from the end of the first round. The warm centrifugation step is repeated in a similar fashion as previously described. Resuspension in cold PBS follows as well as a final cold centrifugation step. The final purified protein is transferred to 50 ml falcon tubes and the purification is complete.

In summary the steps are:

1) Cold Centrifugation
2) Warm centrifugation
3) Pellet re-suspension
4) Cold centrifugation
5) Warm centrifugation
6) Pellet re-suspension
7) Cold Centrifugation

3.4 ELP Purification Supplemented with NaCl

For the ELPs in our library that have transition temperatures above 40 °C ($(GVGVP)_{10}$, $(GVGVP)_{20}$, $(GVGVP)_{10}$-foldon, $(GVGVP)_{20}$ -foldon) the entire purification process is supplemented with 3 M NaCl [48, 58]. The expression follows the same procedure as before. During the purification process, after the pellets were resuspended in BPERII, the samples were supplemented with 3 M NaCl.

3 M NaCl Calculation:

- MW NaCl: 58.4 g
- 3M NaCl = 58.44 g * 3 = 175.32 g into 1 liter
- Convert to milliliters: 175.32 g / 1000 ml = .175g/ml
- Add 3 M NaCl in g/ml to 20 ml sample = .175 g/ml * 20 ml = 3.50 g NaCl into 20 ml resuspended pellet

The subsequent steps are all in 5 ml sample size:

- .175g NaCl * 5 ml = .875 g NaCl into 5 ml samples

The addition of the 3 M NaCl allows the small ELPs to have a transition temperature within the range of our centrifuges. The salt also helps remove other impure proteins from the sample. After the final step, the protein was eluted in 5ml 1X PBS + 3 M NaCl. The samples were then dialyzed in order to ensure that we could control precisely how much salt content was in each of the poly(GVGVP) samples. Dialysis is used to remove salts and other impurities from protein samples. Spectra-Por membranes were used (Spectrum Labs) that had a molecular weight cut-off of 3,500 daltons and a

sample size of 5ml. Dialysis membranes were prepared according to the manufacturers protocol by removing the sodium azide solution and loading the sample with a micro pipette. The dialysis was performed in dH_20 with a magnetic stir bar. The dH_20 was changed 3-4 times over the course of a 24 hour dialysis period. At the end of the dialysis the sample was centrifuged at 10,000g and 4 °C to remove remaining impurities. This procedure was used for the following samples

- $(GVGVP)_{10}$
- $(GVGVP)_{20}$
- $(GVGVP)_{10}$-foldon
- $(GVGVP)_{20}$-foldon

3.5 Procedure for Measuring Protein Concentration

Protein concentrations were determined by using the value of the molar extinction coefficients using a procedure laid out by Gill and von Hippel [11]. The advantage of this method is that we do not need to use a large amount of our protein in order to determine its concentration. Typically protein concentration needs to be measured in its denatured state. The advantage of ELPs is that below their T_t they are in a denatured state already and therefore are ready for measurement. Table 3.1 shows the molar extinction coefficients of model compounds [11].

	Extinction coefficient at wavelength				
Model Compound	**276 nm**	**278 nm**	**279 nm**	**280 nm**	**282 nm**
Tryptophan Trp	5400	5600	5660	5690	5600
Gly-L-Tyr-Gly	1450	1400	1345	1280	1200
Cystine	145	127	120	120	100

Table 3.1: Values of the Molar Extinction Coefficients at Different Wavelengths [11]

We used an ultra violet spectrophotometer (Thermo-Electron Corp) to take the spectral measurements. The absorbance at 280 nm is a program already built into the spectrophotomer which we utilized to take protein concentration measurements. The procedure for taking measurements is as follows:

1. Measure blank sample of 1 ml PBS
2. Make 10 % protein sample in PBS by adding 100 µl protein to 900 µl PBS.
3. Make 5 % - 1.25 % protein sample by removing 500 µl of sample from the cuvette and adding 500 µl PBS.
4. Record measurements and perform the following analysis
5. Determine if the measurements follow a linear decrease, i.e. 5 % concentration measurement should be half of the 10 % concentration measurement.

At this point we are ready to determine the protein concentration. The equation which determines the extinction coefficient of a denatured protein is:

$$\acute{\varepsilon}denatured = a\acute{\varepsilon}\, M,tyr + b\acute{\varepsilon}\, M,\ trp + c\acute{\varepsilon}\, M,\ cys \qquad \textbf{(3.1)}$$

The quantities ε M,tyr, ε M,trp and ε M,cys are the molar extinction coefficients of tyrosine, tryptophan cysteine residues at the wavelengths used. The way to determine this is to look at the amino acid sequence for your protein and count the number of tryptophans, tyrosines and cysteines you have. To determine the protein concentration we then use the following equation, based on Beer's Law.

$$Abs\ denatured\ /\ \acute{\varepsilon}denatured = C\ denatured \qquad \textbf{(3.2)}$$

I will demonstrate the calculation of protein concentration for a $(GVGVP)_n$ sample and a $(GVGVP)_n$-foldon sample. For a sample of $(GVGVP)_n$ the calculation of the molar extinction coefficient is only dependent on the value of the extinction coefficient of tryptophan at 280 nm which is 5690 because the amino acid sequence for $(GVGVP)_n$ only contains one tryptophan residue. The values for $(GVGVP)_{40}$ at different concentrations in PBS are as follows.

Protein Concentration in PBS	Absorbance value @ 280 nm
10 %	.359
5 %	.174
2.5 %	.087
1.25 %	.041

Table 3.2. Protein Concentration determination for $(GVGVP)_{40}$

The calculation of the protein concentration is then as follows:

$$Cden = (.359 / 5690) * 10 * 1000 = .630\ mM \text{ or } 630\ \mu M \qquad \textbf{(3.3)}$$

For a sample of $(GVGVP)_n$-foldon the calculation of the molar extinction coefficient is dependent on the fact that there are two tryptophan residues and two

tyrosine residues, giving a value of the coefficient at 280 nm of 13940. The values for $(GVGVP)_{40}$-foldon in PBS are shown in table 3.3.

Protein Concentration in PBS	Absorbance value @ 280 nm
10 %	1.237
5 %	.570
2.5 %	.260
1.25 %	.116

Table 3.3. Protein Concentration determination for $(GVGVP)_{-40}$-foldon

The calculation of the protein concentration is then:

Cden = (1.237 / 13940) * 10 * 1000 = .880 mM or 880 μM. **(3.4)**

3.6 SDS-PAGE Gel Protocol:

Time course of the expressed proteins (1 ml sample before induction and 1 ml sample after induction) were taken to determine the best strategy for purifying the proteins. Polyacrylamide gel electrophoresis was performed to analyze the samples. The protocol for mini scale bacterial protein extraction is located in the appendix. Briefly, samples are taken pre and post induction to determine the location of the protein. The bacterial pellets are split into soluble and insoluble fractions to determine exactly which step the protein should be located in. The SDS-PAGE gel separates proteins based on their electrophoretic mobility, which results in separation of proteins by size.

3.7 Turbidity Measurements:

All turbidity measurements were made on a Cary Ultraviolet Visible (UV-Vis) Spectrophotometer. The temperature was controlled by a single cell Peltier assembly and a re-circulating water bath. A 10mm path length quartz cuvette was used to house the sample. A small stir bar was placed in the cuvette to perturb the sample. Samples were heated either at 1° C / min or 0.5 ° C / 30 sec at a constant rate. The spectrophotometer produces plots which show the absorbance of light as a function of wavelengths between 200-800 nm. The spectrum was observed throughout the process and the onset of LCST behavior was determined by the spectrum. When a particular temperature caused the plot to exhibit drastically different behavior, such as a much higher slope, the onset of LCST was observed. Measurements were carried out after this onset point until the spectrum became constant again.

After the data was collected the files were exported as an Excel spreadsheet for analysis. Plots were made which showed the absorbance measured at 350 nm versus the temperature. The steep transition is visible at this wavelength [4] and the transition temperature is taken as the midpoint between the onset of turbidity and the resumption of constant absorbance values. Or it is more commonly referred to as half maximal of the turbidity at 350 nm.

We performed experiments on our library of ELPs ranging from 10 repeats to 60 repeats with and without foldon. T_t's were measured as a function of ELP concentration, ELP chain length, and NaCl concentration at a constant ELP concentration.

Chapter IV

Results and Discussion

4. 1 SDS-PAGE Gel Results

This section contains the results and subsequent discussion regarding the SDS-PAGE gel analysis of (GVGVP)n and (GVGVP)n-foldon. The gels were loaded according to the protocol described in the appendix. SDS-PAGE analysis serves 4 main purposes.

1. Determination of molecular weight of protein
2. Quantitative view of protein purity
3. Verify trimer formation of foldon samples
4. Determine thermal stability of foldon samples

The first sample that was completed was the ELP $(GVGVP)_{40}$-foldon sample. We ran an initial gel to determine that the ELP was in the soluble fraction (data not shown) for purification purposes. After the purification of the ELP the thermal stability, trimer

formation and relative purity of $(GVGVP)_{40}$-foldon was investigated. The results are shown in figure 4.1. The gel pictured contains only $(GVGVP)_{40}$-foldon samples.

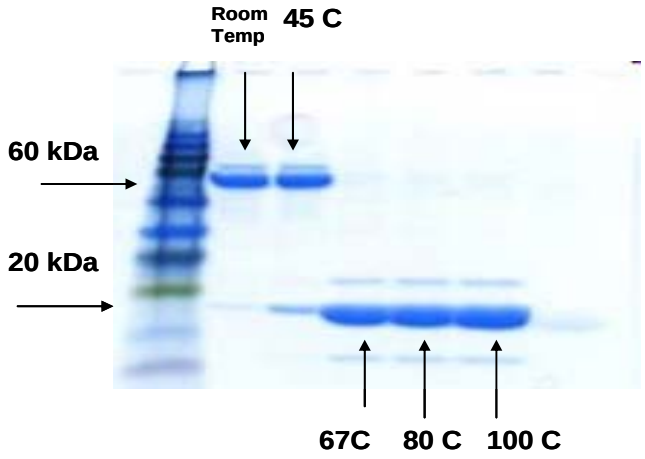

Figure 4.1 SDS-PAGE gel analysis of (GVGVP)40-foldon

On the far left is a full-range molecular weight marker (GE healthcare), which ranges from 12,000-225,00 Da. The expected molecular weight of a $(GVGVP)_{40}$-foldon sample is 20 kDa. All samples were heated prior to loading into the gel using a dry heat bath (Fischer Scientific). The first sample after the molecular weight marker is the construct at room temperature. The band indicates ELP trimer formation by displaying a band at 60 kDa. The sample is also quite pure as there are few impurities visible on the gel. The second band is when the sample is heated to 45 °C. Almost the entire sample remains a trimer, but a small band is visible at the monomer level. The final 3 bands are the construct heated to 67 °C, a temperature just below the thermal stability temperature of the foldon domain [51], 80 °C and 100 °C, two temperatures well above the expected stability level of foldon domain. As anticipated, the foldon domain no longer forms an ELP trimer at these temperatures. This indicates that the foldon domain is only stable up to certain temperatures when attached to ELPs and that we must be conscious of the limits of the domain when designing ELP constructs. Similar procedures were undertaken

with the rest of our ELP samples and each of the foldon constructs maintained their thermal stability up to the temperature limits of the foldon domain. The trimer formation was also verified for each of the samples containing the foldon domain (data not shown).

4.2 Ultraviolet Spectrophotometry Results

This section displays the results of the ultraviolet spectrophotometery studies performed on the library of ELPs used in this study. Samples were prepared for use in the following manner. All samples were pipetted into a quartz cuvette with a 10 mm path length. Sample size was 2 ml and the following calculations were used to determine the amount of protein to use in relation to the amount of buffer. For the following group of proteins, all samples were measured in PBS, while varying the ELP concentration.

$(GVGVP)_{60}$-foldon

$(GVGVP)_{40}$-foldon

$(GVGVP)_{40}$

In order to determine the transition temperatures (T_t's) we used an ultra violet spectrophotometer to measure the onset of turbidity in our samples. The concentration of the ELPs ranged from 5 μM to 400 μM depending on the initial sample concentration. We are expecting to see a decrease in the T_t with an increase in ELP concentration. This trend has been reported in literature previously [34,67,68]. We also expect to see lower T_t values for trimerized $(GVGVP)_n$-foldon, than for linear $(GVGVP)_n$ constructs. It has previously been reported that the foldon domain will increase the thermal stability of collagen like proteins [51, 53]. Another hopeful result of this study is that $(GVGVP)$-$_n$-

foldon samples will show protein concentration independence [51], as compared to the strong concentration dependence reported for ELPs [34,67,68].

The oligomerization domain has the ability to cause the ELPs to form trimers. Therefore a sample of $(GVGVP)_{10}$-foldon should have the same molecular weight as a linear $(GVGVP)_{30}$. Therefore an ELP containing the foldon domain should follow the same molecular weight dependent decrease on the T_t as reported for linear ELPs but in a more dramatic fashion. The T_t's for short linear ELPs (5-15 repeats) are very high (100-120 °C) according to extrapolations performed in literature [58, 67]. Typically the values for the T_t for these short ELPs are higher than the measuring capabilities of UV-vis spectrophotometers used to measure turbidity. Alternatively the addition of NaCl at various concentrations has been shown to lower the T_t to measurable values as well. For the short ELPs with attached foldon domain we hope to impart the characteristics of a larger ELP in terms of T_t values.

An example of the raw data that is given by the UV-spec is shown in figure 4.2. It is representative of the $(GVGVP)_{40}$ sample at an ELP concentration of 5 μM. Data is reported as absorbance at 350 nm wavelength versus temperature. We take the transition temperature to be point of one-half of the maximal turbidity.

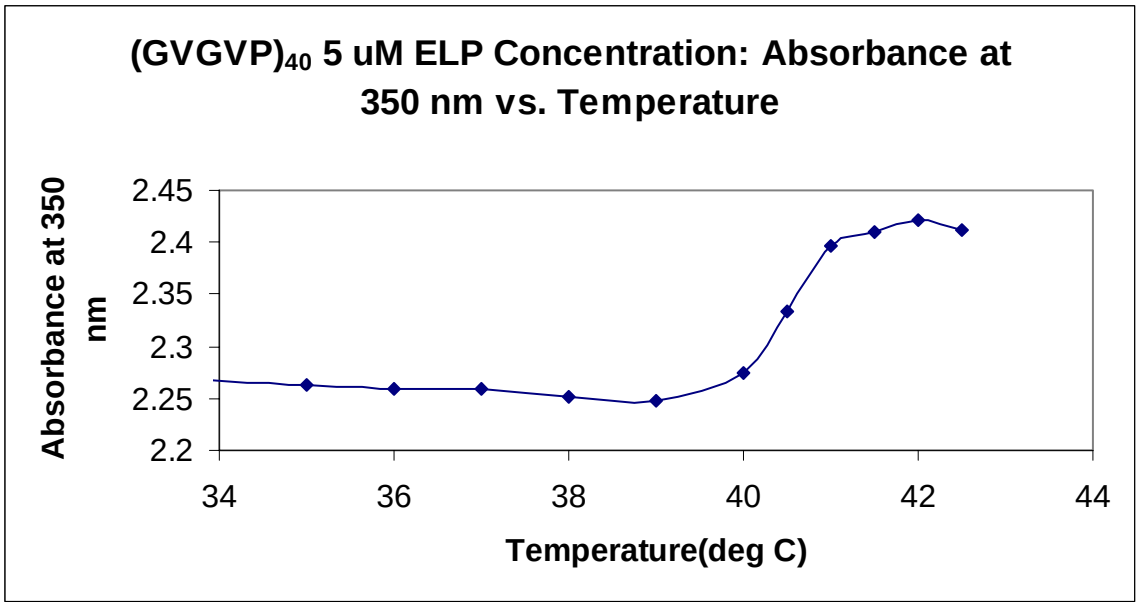

Figure 4.2 Data from UV-Spectrophotometer given as a function of absorbance at 350 nm

Transition temperature determined from this figure would be done in the following manner. The point where the slope begins to change to a strong upward curve is at an absorbance value of 2.24 nm and the point where the slope changes back is at an absorbance value of 2.42. Taking the mid-point between the two will give the point where the slope is changing most rapidly, or the maximum of the derivative. Finding the temperature that corresponds to the midpoint value of the absorbance is the transition temperature. In equation form:

$$\frac{Abs_{(onset)} + Abs_{(end)}}{2} = T_t \qquad \textbf{(4.1)}$$

For this data set then the calculation would be: 2.24 + 2.42 / 2 = 2.33. An absorbance value of 2.33 corresponds to a transition temperature of 40.2 °C. This process is repeated for all UV spectrophotometry measurements.

4.3 T_t vs. ELP Concentration

Figures 4.3-7 show the results of the each sample's T_t profile as a function of ELP concentration. It has been reported that T_t decreases with increasing ELP concentration up to a certain "concentration limit" [68]. This has been confirmed with our results. There is a larger variation in T_t values for lower protein concentrations than for higher protein concentrations. These results hold true for both the linear $(GVGVP)_n$ and the modified $(GVGVP)_n$-foldon samples. A possible explanation for this is that the foldon domain has a greater effect on the T_t values at lower ELP concentrations due to the fact that it increases the intrinsic concentration of the sample [51]. The small volume of the foldon domain and the increased hydrophobic interactions, when attached to an ELP of low concentration, can have a somewhat similar effect of increasing the overall hydrophobicity of the ELP. When the overall hydrophobicity of the ELP is increased the T_t decreases as well [4]. Another explanation of these effects is that since the foldon domain creates ELP trimers the expected effects of T_t decrease with increasing molecular weight will be seen. Therefore a $(GVGVP)_{40}$-foldon ELP will have a higher molecular weight than a $(GVGVP)_{40}$ and thus will have a lower T_t [34]. This is a multi-variant effect, however, and thus a trimerized $(GVGVP)_{40}$-foldon will not necessarily follow the patterns of T_t decrease with increasing chain length [67]. Thus a trimerized $(GVGVP)_{40}$-foldon will not behave like a linear $(GVGVP)_{120}$, nor will it behave like a $(GVGVP)_{40}$. The effects are unique and not yet fully understood.

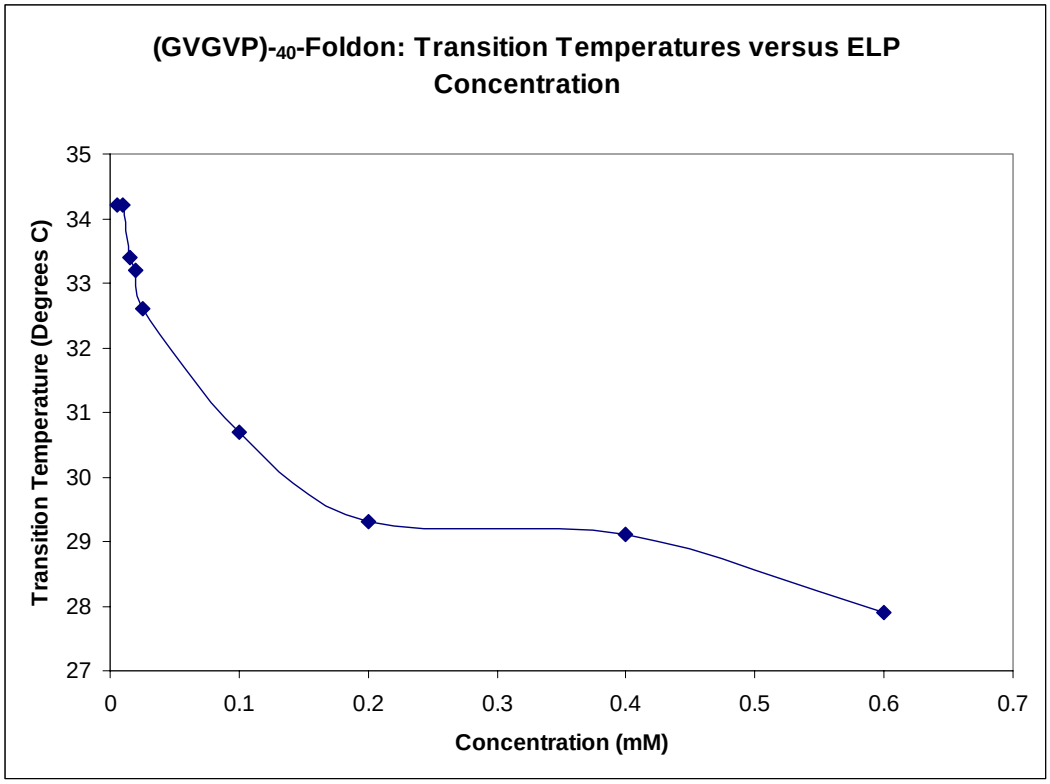

Figure 4.3. $(GVGVP)_{40}$-foldon: Transition temperature versus ELP concentration

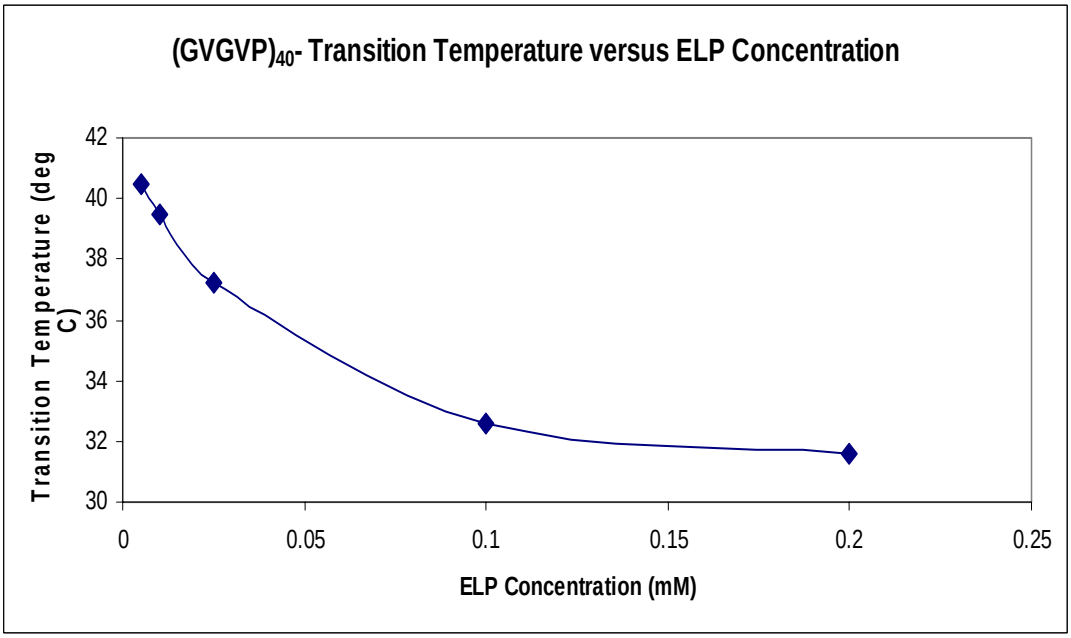

Figure 4. 4. GVGVP-40 Transition Temperature versus ELP concentration

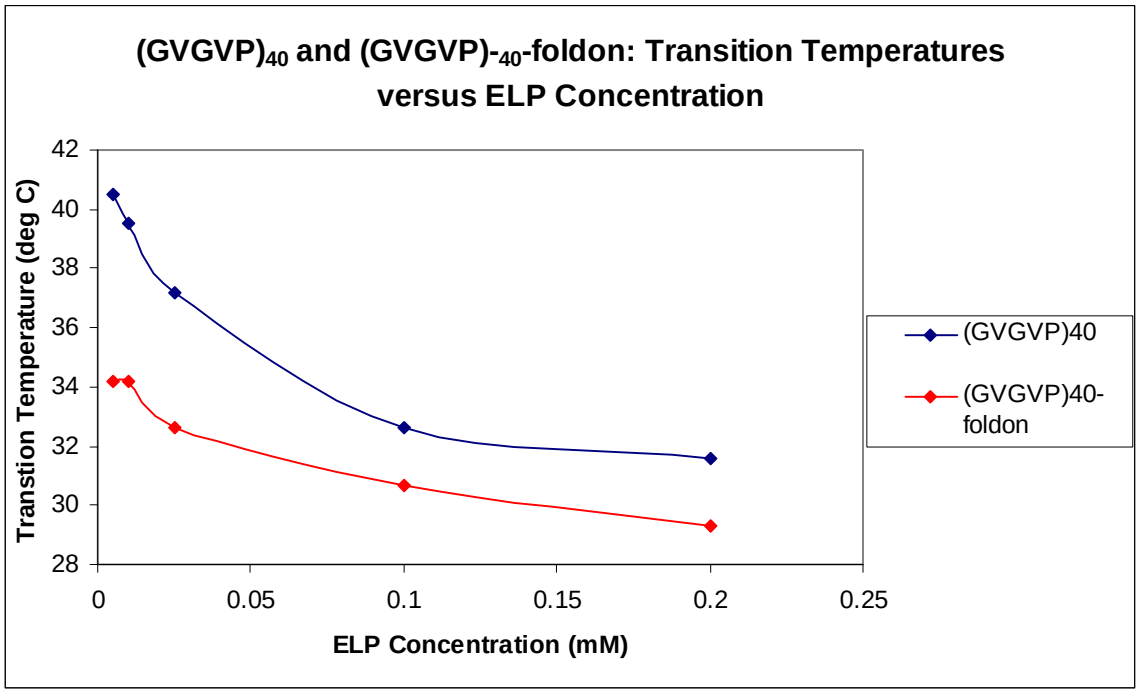

Figure 4. 5. $(GVGVP)_{40}$ and $(GVGVP)_{40}$-foldon: A comparison between the foldon and linear $(GVGVP)_{40}$ samples at various ELP concentrations

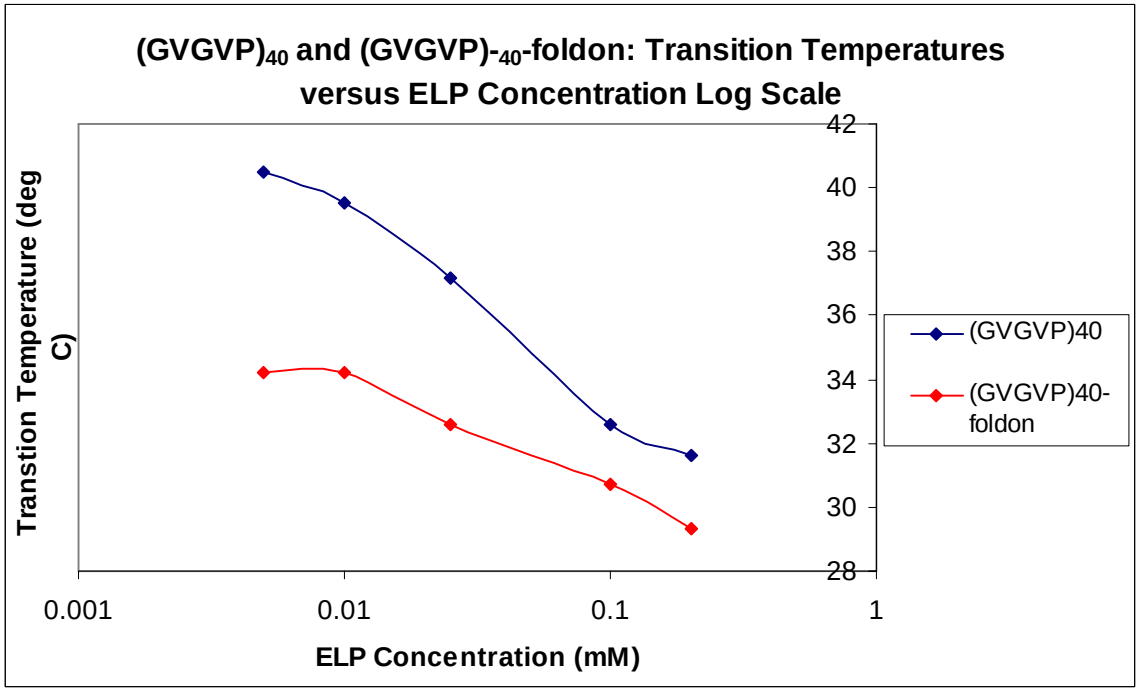

Figure 4. 6. $(GVGVP)_{40}$ and $(GVGVP)_{40}$-foldon: A comparison between the foldon and linear $(GVGVP)_{40}$ samples at various ELP concentrations

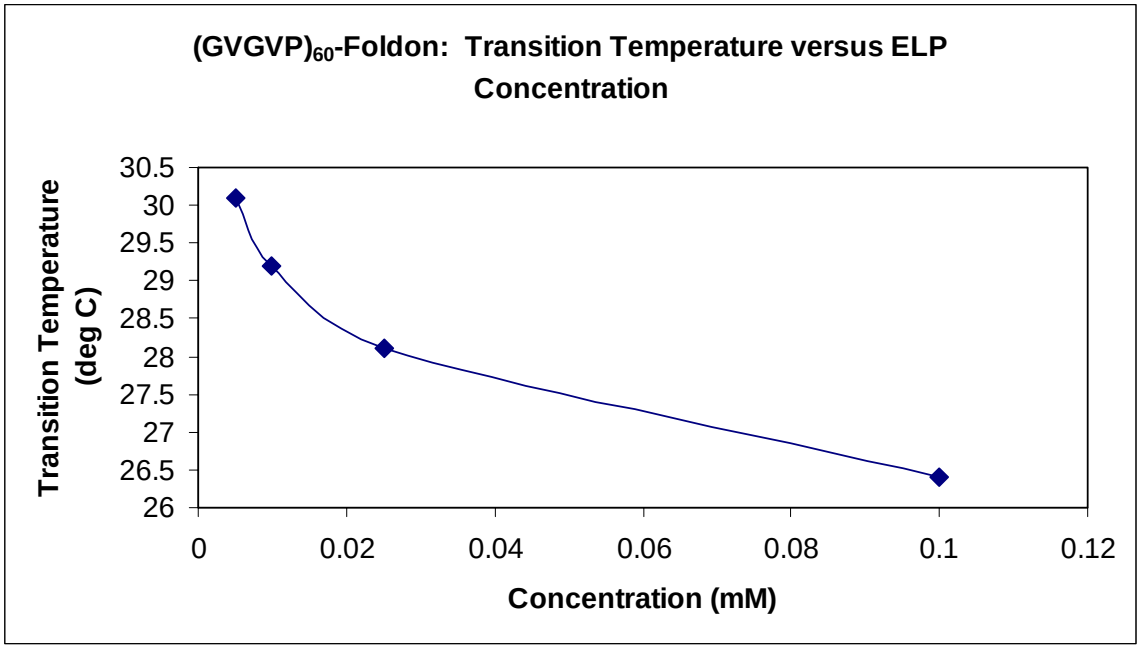

Figure 4. 7. (GVGVP)60-Foldon transition temperature versus ELP concentration

Figure 4.5 shows a comparison between $(GVGVP)_{40}$ and $(GVGVP)_{40}$-foldon. It can be clearly seen from the results that the ELPs with foldon domain have lower transition temperatures than ELPs without foldon for all concentrations. This is in line with what we were expecting to see. However, we can not say that the addition of the foldon domain renders the ELP concentration independent. Even though $(GVGVP)_{40}$ foldon had the same T_t at ELP concentrations of 5μM and 10 μM, the values at 15 and 20 μM were different by 1 °C each. It is not possible to say that this means there is concentration independence by these results. At very low concentrations the foldon domain may increase the intrinsic concentration enough to narrow the effects of concentration, but as the concentration of the ELP gets larger the T_t begins to decrease according to expected results [68]. This is most likely due to the fact that the foldon domain will have its greatest effect on very small chains and at very low ELP

concentrations. By bringing the expected ELP triple strands in close proximity, the foldon domain will exact the most striking effects when the chain lengths are small and the concentration is already low. However as the chains increase in length and the ELP concentration increases the effects of the foldon domain are mitigated. Figure 4.6 is another comparison between $(GVGVP)_{40}$ and $(GVGVP)_{40}$-foldon, and this time the data is plotted on a logarithmic scale in regards to concentration. The slope of the $(GVGVP)_{40}$-foldon sample is less steep and begins to flatten out in comparison to the $(GVGVP)_{40}$ sample at low concentrations. This plot is encouraging in terms of achieving concentration independence at very low ELP concentrations for ELPs containing the oligomerization domain.

4.4 T_t as a Function of Chain Length

Figures 4.8 and 4.9 show the variation of T_t with ELP chain length at a constant ELP concentration of 25 μM. The effects of chain length on the T_t for $(GVGVP)$-$_n$-foldon are striking. By doubling the number of repeats we are able to reduce the T_t by 47.8 °C. This is a dramatic change and can be explained by the trimerizing mechanism of the foldon domain. The values used for the linear $(GVGVP)_n$ samples came from literature except for $(GVGVP)_{40}$, which we were able to measure. The reason for this is, although we were able to successfully synthesize and verify through sequencing the $(GVGVP)_{10}$ and $(GVGVP)_{20}$ constructs, the expression and purification stages were unable to be successfully completed. For reasons unknown at this time, we had such low yields of ELP protein at the conclusion of these stages that they not usable. The $(GVGVP)_{60}$ construct was unable to be synthesized. After repeated efforts, I was never able to

successfully synthesize that particular construct. Thus the values for the T_t of GVGVP-(10,20 and 60) come from Chilkoti et al. [67]. The values taken were all GVGVP samples at 25 μM concentration in PBS.

The differences between the $(GVGVP)_n$ and $(GVGVP)_n$-foldon constructs are shown in figure 4.9 and in table 4.1. As expected, for shorter chain lengths we had very high T_t values for both constructs. For small constructs, 10 and 20 repeat units there is a large difference in ΔT_t for both constructs. The effects of the foldon domain are again, the largest for small chain lengths. This is similar to the concentration effects and the solution parameter effects. As the ELP construct gets larger the effects begin to plateau and the differences between constructs becomes less noticeable. However, the (GVGVP)-foldon constructs still have lower T_t values across all values. This indicates that although the effects are larger for smaller constructs, the foldon domain still impacts the larger chains.

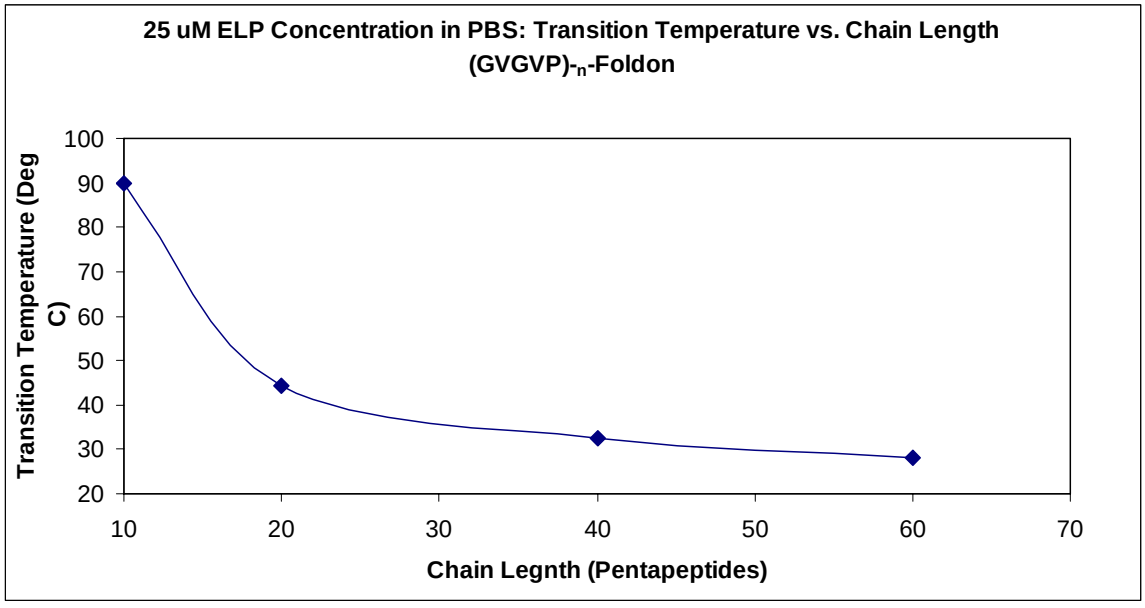

Figure 4.8: T_t as a function of chain length for $(GVGVP)_n$-foldon

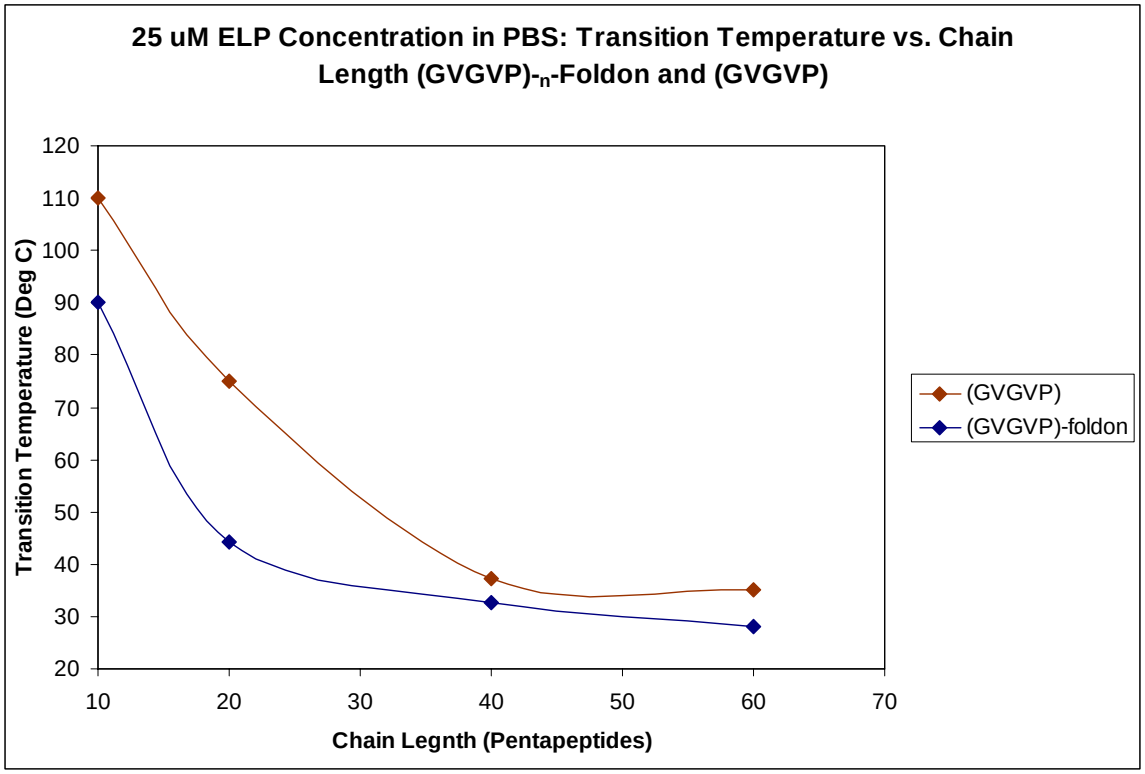

Figure 4.9: T_t as a function of Chain Length: $(GVGVP)_n$ and $(GVGVP)$-$_n$-foldon ELPS @25 µM ELP concentration

Chain Length	Transition Temperatures (°C) 25 µM samples in PBS		
	$(GVGVP)_n$	GVGVP-foldon	ΔT_t
10	110	90	20
20	75	47.8	27.2
40	37.2	32.6	4.6
60	35	28.1	6.9

Table 4.1: Comparison between linear $(GVGVP)_n$ T_t values from literature and measured $(GVGVP)$-$_n$-foldon samples.

4.5 T_t as a Function of Solution Properties

This section describes how the T_t changes with solution parameters for ELPs. Specifically we alter the concentration of NaCl in the solution and observe the effects on the T_t. As previously described the samples were all dialyzed so as to be in an essentially pure water state. From this point we were able to specifically control the amount of NaCl that was present in the sample. The first step was to make 1 liter of 3 M NaCl PBS, by the addition of 175.32 g of NaCl to PBS. The second step was to determine a way to control the protein concentration. Similar to the literature, we chose 25 μM as a constant ELP concentration. The creation of an excel sheet was undertaken which allowed for the variation of only the NaCl concentration by keeping the ELP concentration constant.

The addition of NaCl is necessary to measure the transition temperature for (GVGVP)-$_{10}$-foldon and is included for (GVGVP)-$_{20}$-foldon. (GVGVP)-$_{10}$-foldon at 0 M NaCl concentration has a T_t above 70 °C°, which is above the thermal stability temperature of the foldon domain [51], but is measured regardless. It should have the expected T_t of a linear $(GVGVP)_{10}$. As expected shorter chain lengths have higher T_t than longer chain lengths at the same concentration. Also when we increase the NaCl concentration the T_t decreases in a mainly linear fashion.

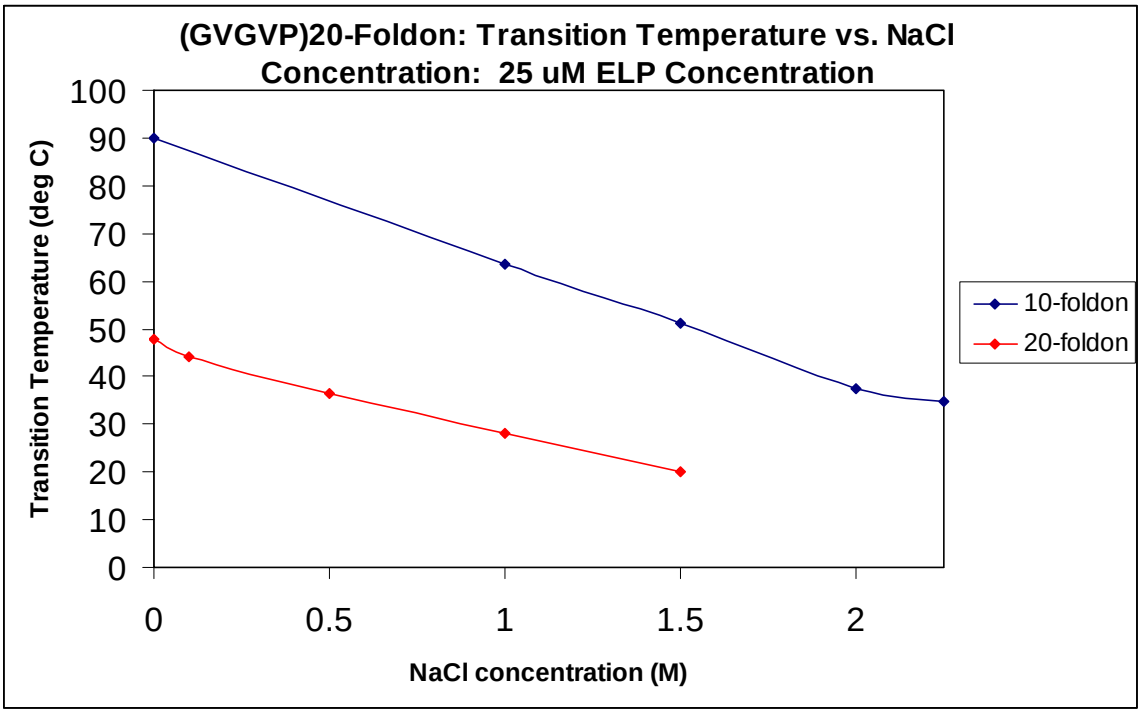

Figure 4.10. Comparison of $(GVGVP)_{20}$- foldon and $(GVGVP)_{10}$-foldon T_t vs. NaCl concentration at a constant ELP concentration of 25 µM

For $(GVGVP)_{10}$-foldon and $(GVGVP)_{20}$-foldon we see an expected linear decrease in T_t with the addition of higher concentrations of NaCl, which is shown in figure 4.10. The effects of the NaCl addition lead to smaller differences in T_t values as the NaCl concentration increase. In $(GVGVP)_{10}$-foldon the T_t begins to reach a plateau as the NaCl concentration goes increases from 2M to 2.25M. This is most likely due to a limiting effect. Additional salts would only lead to a process of salting out of the proteins according to what we have seen on the SDS-PAGE gel results.

In figure 4.11 the T_t of a $(GVGVP)_{40}$ sample was measured as a function of NaCl concentration. The measured T_t values undergo a sharp decline with addition of NaCl. The effct of the addition of 0.75 M NaCl causes the ELPs T_t to drop below room temperature to a value of 24.2 °C. This T_t value is not really of practical value as an T_t below room temperature is not very useful in applications. However, I believe it

illustrates an important point about the multi-variant effects of chain length, molecular weight and solution parameters. For all ELPs there appears to be a limit to the variation of T_t values. When you have larger ELPs the T_t variation window becomes smaller and the effects of changes can lead to the loss of practical applicability. Too much NaCl will drive the T_t of an ELP $(GVGVP)_{40}$ from a physiological range to an unworkable range. However an ELP $(GVGVP)_{10}$-foldon requires the addition of 2M NaCl to affect a T_t change from useless to within a physiological range. However increased addition beyond 2M will eventually lead to the inability to change the T_t values.

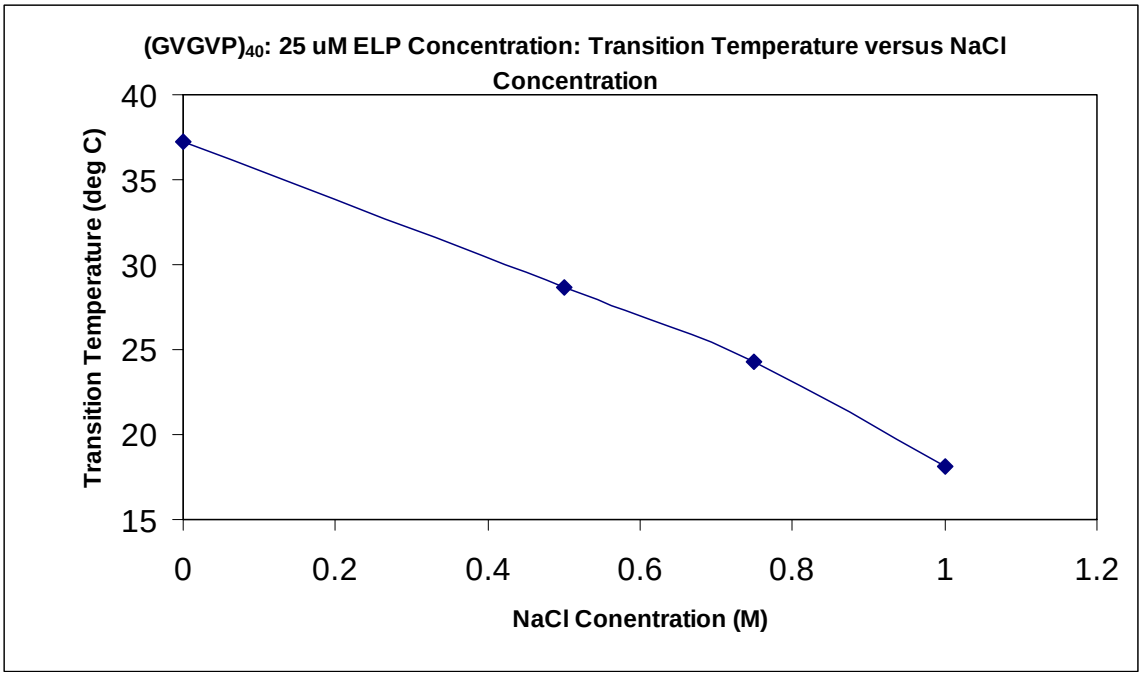

Figure 4.10 $(GVGVP)_{40}$: T_t as a function of NaCl concentration

Chapter V

Summary

We were able to successfully synthesize a library of ELP constructs with an attached oligomerization domain in order to investigate its effects on LCST behavior. The addition of oligomerization domains to ELPs effectively creates trimers which causes a change in the LCST behavior of the constructs. The results showed that for all ELP constructs, the samples with attached foldon domain showed lower T_t values across a range of chain lengths, ELP concentrations and solution parameters. The effects of the foldon domain were seen to be the most substantial at small ELP chain lengths and low ELP concentrations. These effects are in line with the theory of ELPs that concentration and chain length have greater effects on the T_t at low ELP concentrations and small chain lengths. There are many possible explanations for the impact of the foldon domain. The first is that since the trimerizing mechanism increases the molecular weight of the ELP 3-fold the addition of a foldon domain will have similar effects to increasing the molecular weight of ELPs. Thus it is possible to have enhanced effects on small ELP chain lengths.

The second theory is that due to the extensive hydrophobic interactions present within the foldon domain the attachment of this domain to ELPs is similar to increasing the overall hydrophobicity of the ELP, which is known to reduce the T_t. Finally, the trimerizing mechanism imparts some increase on the ELP chain length, though this is not fully understood. The results do not show trimerizing behavior of the the foldon domain do not have exact T_t values as the linear ELPs they are replicating. Thus, although a $(GVGVP)_{20}$-foldon should behave exactly like a $(GVGVP)_{60}$ construct, this is not the case. The overall effect of the foldon domain on ELPs is multi-variant and dependent on many of the same factors as linear ELPs.

The ability to synthesize ELPs with an attached foldon domain is advantageous for two reasons. The first is that it adds an additional element that is able to tune the T_t of ELPS to desired values. This allows us to create new constructs, which take advantage of the foldon domain and expand our ability to make fully tunable ELPs. The second advantage is that we are able to rapidly expand the size and variability of our ELP library. Due to the difficult and unpredictable nature of ELP recursive directional synthesis, our ability to keep expanding the library consistently faces challenges. By attaching a foldon domain to ELPs, we are able to create constructs of large effective sizes and thus increase the overall size of our ELP library. This is useful again for being able to create ELP constructs tuned to specific conditions.

By understanding how to synthesize and fully characterize ELPs with and without the foldon domain we will be able to create responsive materials in the future that can be suitable for a wide range of applications.

BIBLIOGRAPHY

[1] J. Cabello-Rogdriguez, S. Prieto, Biofunctional design of elastin-like polymers for advanced applications in nanobiotechnology, *Journal of Biomaterial Science Polymer Edition,* 18 **(2006)** 269.

[2] D. Chow, D.W. Lim, Peptide-based biopolymers in biomedicine and biotechnology. *Materials Science and Engineering,* 62 **(2008)** 155.

[3] J. Reguera, A. Girotti, Developing functionality in elastin-like polymers by increasing their molecular complexity: the power of the genetic engineering approach, *Progress in Polymer Science.* 30 **(2005)** 1145.

[4] D.W. Urry, Physical Chemistry of Biological Free Energy Transduction as Demonstrated by Elastic Protein-Based Polymers, *Journal of Physical Chemistry,* 101 **(1997)** 1128.

[5] L.B. Sandber, N.T. Soskel, J.B. Leslie, Elastin Structure Biosynthesis and Relation, *New England Journal of Medicine,* 304 **(1981)** 579.

[6] D.W. Urry, Entropic Elastic Processes in Protein Mechanisms. I Elastic Structure Due to an Inverse Temperature Transition and Elasticity due to Internal Chain Dynamics, *Journal of Protein Chemistry.* 7 **(1988)** 34.

[7] J. Rodriguez-Cabello, M. Alonso, T. Perez, M.M Herguedas, Differential Scanning Calorimetry Study of the Hydrophobic Hydration of the Elastin-Base Pentapeptide, Poly(GVGVP), from Deficiency to Excess of Water, *Biopolymers,* 54 **(2000)** 288.

[8] D.W. Urry, T. L. Trapane, Phase-Structure Transitions of the Elastin Polypentapeptide-Water System Within the Framework of Composition-Temperature Studies, *Biopolymers,* 24 **(1985)** 2356.

[9] L. H. Sperling, *Introduction to Physical Polymer Science.* Fourth edition ed. Wiley: 2006.

[10] D.W. Urry, D.T. McPherson, J. Xu, Prodcut Purification by Reversible Phase Transition Following *Escheria Coli* expression of Genes Encoding up to 251 Repeats of the Elastomeric Pentapeptide GVGVP, *Protein Expression and Purification,* 7 **(1996)** 57.

[11] G. Walsh, *Proteins Biochemistry and Biotechnology.* 1st edition ed. Wiley: 2002.

[12] D. Kurkov, P. Schmidt, J. Dybal, J.C. Rodriguez-Cabello, M. Alonso, Structure and Dynamics of Two Elastin-like polypentapeptide Studied by NMR Spectroscopy, *Macromolecules,* 4 **(2003)** 601.

[13] D. Kurkova, J.C. Rodriguez-Cabello, J. Kriz, F.J. Arias, NMR Study of the cooperative behavior of themotropic model polypeptides, *Polymer International,* 56 **(2007)** 194.

[14] J. Dybal, P. Schmidt, J. Kriz, M. Alonso, D. Kurkova, Role of Hydration in the phase transition of polypeptides investigated by NMR and Raman Spectroscopy, *Macromolecular Symposia,* 205 **(2004)** 150.

[15] R. Glaves, M. Baer, E. Schreiner, Conformational Dynamics of Minimal Elastin-like Polypeptides: The role of Proline Revealed by Molecular Dynamics and Nuclear Magnetic Resonance, *ChemPHYSChem,* 9 **(2005)** 2765.

[16] D. W. Urry, T.L. Trapane, R.B McMichens, R.D. Harris, K. U. Prasad, Nitrogen-15 NMR Relaxation Study of Inverse Temperature Transitions in Elastin Polypentapeptide and Its Cross-Linked Elastomer, *Biopolymers,* 25 **(1986)** 228.

[17] B. Bohicchio, A. Pepe, A.M Tamburro, Investigating by CD the Molecular Mechanism of Elasicity of Elastomeric Proteins, *Chirality,* 20 **(2008)**, 994.

[18] B. Bohicchio, A. Pepe, A.M Tamburro, Dissection of human tropoelastin: exon by exon chemical synthesis and related conformational studies, *Biocehmistry,* 42 **(2003)** 13362.

[19] P. Schmidt, J. Dybal, J.C. Rodriguez-Cabello, V. Reboto, Role of Water in Structural Changes of Poly(AVGVP) and Poly(GVGVP) Studied by FTIR and Raman Spectroscopy and ab Initio Calculations, *Biomacromolecules,* 6 **(2005)** 706.

[20] J. Reguera, J.M Lagarn, M. Alonso, B. Calvo, J.C. Rodriguez-Cabello, V. Reboto, Thermal Behavior and Kinetic Analysis of the Chain Unfolding and Refolding and of the Concomitant Nonpolar Solvation and Desolvation of Two Elastin-like Polymers, *Macromolecules,* 36 **(2003)** 8476.

[21] C. Tanford, How Protein Chemists Learned about the hydrophobic factor, *Protein Science,* 6 **(1997)** 1366.

[22] B. Li, O. Darwin, A. Alonso, B.J Bennion, V. Dagget, Hydrophobic Hydration is an Important Source of Elasticity in Elastin-Based Biopolymers, *Journal of the American Chemical Society,* 123 **(2001)** 11998.

[23] A. Krukau, I. Brovchenko, A. Geiger, Temperature Induced Conformational Transition of a Model Elastin-like Peptide GVP(VPGVG) in Water, *Biomacromolecules,* 8 **(2007)** 2202.

[24] M. Baer, E. Schreinere, A. Kohlmeyer, R. Rosseau, D. Marx, Inverse Temperature Transition of a Biomimetic Elastin Model: Reactive Flux Analysis of Folding/Unfolding and its Coupling to Solvent Dielectric Relaxation, *Journal of Physical Chemistry B.* 110 **(2006)** 3587.

[25] P. Schmidt, J. Dybal, J.C. Rodriguez-Cabello, M. Alonso, Raman Spectroscopy of secondary structure of elastinlike polymer poly(GVGVP), *Biopolymers,* 62 **(2001)** 157.

[26] J.C. Rodriguez-Cabello, M. Alonso, M. Diez, M. Caballero, M. Herguedas, Structural Investigation of the poly(pentapeptide) of elastin, poly(GVGVP) in the solid state, *Macromolecular Chemistry and Physics*, 200 **(1999)** 1838.

[27] A. Chilkoti, T. Christensen, J.A. MacKay, Stimulus Responsive elastin biopolymers: applications in medicine and biotechnology, *Current Opinion in Chemical Biology,* 10 **(2006)** 657.

[28] R. Yerushalmi, A. Scherz, M.E. van der Boom, H-B. Kraatz, Stimuli responsive materials: new avenues toward smart organic devices, *Journal of Materials Chemistry,* 15 **(2005)** 4487.

[29] A. Chilkoti, N.Nath, Creating "Smart" Surfaces Using Stimuli Responsive Polymers, *Advanced Materials,* 14 **(2002)** 1246.

[30] D.W. Urry, T.M. Parker, Biocompatibilty of the Bioelastic Materials, Poly(GVGVP) and its γ-Irradiation Cross-Linked Matrix: Summary of the Generic Biological Test Results, *Journal of Bioactive and Compatible Polymers,* 6 **(1991)** 282.

[31] D.W. Urry, A. Nicol, *Biotechnological Polymers: Medical, Pharmaceutical and Industrial Applications,* **(1993)** 82.

[32] T. Yamaoka, A. Panitch, D.A. Tirrell, Design and Biosynthesis of elastin-like extracellular matrix proteins containing periodically spaced fibronectin CS5 domains, *Macromolecules,* 32 **(1999)** 1703.

[33] A. Chilkoti, D.E. Meyer, Characterization of a Genetically Engineered Elastin-like Polypeptide for Cartilaginous Tissue Repair, *Biomacromolecules,* 3 **(2002)** 916.

[34] A. Girotti, J. Reguera, Influence on the Molecular Weight on the Inverse Temperature Transition of a Model Genetically Engineered Elastin-like pH Responsive Polymer, *Macromolecules,* 37 **(2004)** 3400.

[35] A. Chilkoti, D.W. Lim, Rapid Cross-Linking of Elasin-Like Polypeptides with (Hydroxymethyl)phosphines in Aqueous Solution, *Biomacromolecules,* 8 **(2007)** 1470.

[36] D.W. Lim, D.L. Nettles, In Situ Cross-Linking of Elastin-like Polypeptide Block Copolymers for Tissue Repair, *Biomacromolecules,* 9 **(2008)** 230.

[37] N. Nath, J. Hyun, Capture and Release of Proteins on the Nanoscale by Stimuli-Responsive Elastin-like polypeptide "Switches", *Journal of American Chemical Society,* 126 **(2004)** 735.

[38] A. Valiaev, N. Anu-Lail, Microcantilever Sensing and Actuation with End-Grafted Stimulus-Responsive Elastin-like Polypeptides, *Langmuir,* 23 **(2007)** 344.

[39] A. Valiaev, T. Oas, A. Chilkoti, Force-Induced Prolyl Cis-Trans Isomerization in Elastin-like Polypeptides, *Journal of American Chemical Society,* 129 **(2007)** 6497.

[40] T. Hugel, D.W. Urry, M. Seitz, H.E. Gaub, Elastin: a representative ideal protein elastomer, *Philosophical Transactions of the Royal Society of London Biological Sciences,* 357 **(2002)** 184.

[41] A. Simnick, D.W. Lim, D. Chow, Biomedical and Biotechnological Applications pf Elastin-Like Polypeptides, *Journal of Macromolecular Science,* 47 **(2007)** 154.

[42] D.E. Meyer, A. Chilkoti, G.A. Kong, Targetting a genetically engineered elastin-like polypeptide to solid tumors by local hypothermia, *Cancer Research,* 61 **(2001)** 1554.

[43] J. Cappello, J. Crissman, Genetic Engineering of Structural Protein Polymers, *Biotechnology Progress,* 6 **(1990)** 202.

[44] A. Nagareskar, J. Crissman, Genetic Synthesis and Characterization of pH and temperature sensitive silk-elastinlike protein block copolymers, *Journal of Biomedical Materials Research,* 62 **(2002)** 203.

[45] J. Cappello, D.Q. Li, M. Haider, In vitro and In vivo evaluation of recombinant silk-elastinlike hydrogels for cancer gene therapy. *Journal of Controlled Release,* 94 **(2004)** 445.

[46] M. Haider, J. Cappello, K.W. Leong, In vitro chondrogenesis of mesenchymal stem cells in recombinant silk-elastinlike hydrogels, *Pharmaceutical Research,* 25 **(2008)** 699.

[47] H. Lodish, D. Baltimore, A. Berk, S.L. Zipursky, P. Matsudaira, J. Darnell, *Molecular Cell Biology,* Third Edition ed.; Scientific American: 1995

[48] D.E. Meyer, A. Chilkoti, Genetically Encoded Synthesis of Protein-Based Polymers with Precisely Specified Molecular Weight and Sequence by Recursive Directional Ligation: Examples from the Elastin-like Polypeptide System, *Biomacromolecules,* 3 **(2002)** 367.

[49] Y. Tao, S. Strelkov, M.G. Rossman, V. Mesyanzhinov, Structure of bacteriophage T4 fibritin: a segmented coiled coil and the role of the C-terminal domain, *Structure,* 15 **(1997)** 798.

[50] J. Engel, R. Kammerer, What are Oligomerization domains good for?, *Matrix Biology,* 19 **(2000)** 288.

[51] S. Frank, r. Kammerer, D. Mechling, T. Schulthess, R. Landwehr, J. Bann, Y. Guo, A. Lustig, H.P. Bachinger, J. Engel, Stabilization of Short Collagen-like Triple Helices by Protein Engineering, *Journal of Molecular Biology,* 308 **(2001)** 1089.

[52] J. Stetefeld, S. Frank, M. Jenny, T. Shculthess, R. Kammerer, S. Boudko, R. Landwehr, K. Okuyama, J. Engel, Collagen Stabilization at Atomic Level: Crystal Structure of Designed (GlyProPro)10foldon, *Structure,* 11 **(2003)** 346.

[53] C. Du, M. Wang, J. Liu, M. Pan, Y. Cai, J. Yao, Improvement of Thermostability of recombinant collagen-like protein by incorporating a foldon sequence, *Applied Microbiology Technology,* 79 **(2008)** 202.

[54] S. Meier, S. Guthe, T. Kiefhaber, S. Grzesiek, Foldon, the Natural Trimerization Domain of T4 Fibritin, Dissociates into a Monomerica A-state Form containing a Stable β-Hairpin: Atomic Details of Trimer Dissociation and Local β-Hairpin Stability from Residual Diploar Couplings, *Journal of Molecular Biology,* 344 **(2004)** 1069.

[55] B.N. Sobolev, M.M. Shneider, E.I. Maruisch, V.V. Mesyanzhinov, Fibritin and adhesion of bacteriophage T4 tells us how fibrous protein folds and assembles, *Evolutionary Biochemistry and Related areas of Physiochemical Biology,* **(1995)** 374.

[56] J. Reguera, D.W. Urry, T.M. Parker, D.T. McPherson, J.C. Rodriguez Cabello, Effect of NaCl on the Exothermic and Endothermic Components of the Inverse

Temperature Transition of a Model Elastin-like Polymer, *Biomacromolecules,* 8 **(2007)** 358.

[57] J. Reguera, D.W. Urry, T.M. Parker, D.T. McPherson, J.C. Rodriguez Cabello Endothermic and Exothermic Components of an Inverse Temperature Transition for hydrophobic association by TMDSC, *Journal of Chemical Physical Letters,* 388 **(2004)** 131.

[58] H. Nuhn, H.A. Klok, Secondary Structure Formation and LCST Behavior of Short Elastin-Like Peptides, *Biomacromolecules,* 9 **(2008)** 2763.

[59] D.W. Urry, M. Long, H. Sugano, Cyclic Analog of elastin polyhexapeptide exhibits an inverse temperature transition leading to crystallization, *Journal of Biological Chemistry,* 253 **(1978)** 6302.

[60] M. Pechar, J. Brus, L. Kostka, C. Konak, Thermoresponsive self-assembly of short elastin-like polypentapeptides and their poly(ethylene glycol) derivatives, *Macromolecular Bioscience,* 7 **(2007)** 59.

[61] J.C. Van Hest, L. Ayres, K. Koch, P. Adams, Stimulus Responsive Behavior of Elastin-Based Side Chain Polymers, *Macromolecules,* 38 **(2005)** 1704.

[62] C.H Luan, T.M Parker, D.W. Urry, K.U Prasad, Differential scanning calorimetry studies of NaCl effects on the inverse temperature transition of some elastin-based polytetra, polypenta and polynonapeptides, *Biopolyers,* 31 **(1991)** 475.

[63] T. Yamaoka, T. Tamuar, Y. Seto, T. Tada, S. Kunugi, D. Tirrell, Mechanism for the Phase Transition of a Genetically Engineered Elastin Model Peptide (VPGIG)40 in Aqueous Solution, *Biomacromolecules,* 4 **(2003)** 1685.

[64] Y. Zhang, K. Trabbic-Carlson, F. Albertorio, A. Chilkoti, P.S. Cremer, Aquesous Two-Phase System Formation Kinetics for Elastin-like Polypeptides of Varying Chain Length, *Biomacromolecules,* 7 **(2006)** 2199.

[65] P.H. Von Hippel, K.Y. Wong, On the conformational stability of globular proteins. The effects of various electrolytes and nonelectrolytes on the themal ribonuclease transition, *Journal of Biological Chemistry,* 240 **(1965)** 3923.

[66] D. W. Urry, T. L. Trapane, K.U. Prasad, Phase-Structure Transitions of the Elastin Polypentapeptide-water system Within the Framework of Composition-Temperature Studies, *Biopolymers,* 24 **(1985)** 2356.

[67] D.E. Meyer, A. Chilkoti, Quanitification of the Effects of Chain Length and Concentration on the Thermal Behavior of Elastin-like Polypeptides, *Biomacromolecules,* 5 **(2004)** 851.

[68] D.W. Urry, Molecular Machines: how motion and other functions of living organisms can results from reversible chemical changes, *Angew Chem Int Ed Engl,* 32 **(1993)** 841.

APPENDIX

A.1 Procedure for Monitoring Cell Densities and Inducing Proteins

- Take 1 mL sample and put into cuvettes used for cell density measurements (>600 nm)
- **Measuring Cell Densities**
    1. Go to UV Spectrophotometer
    2. Select Cell Growth Program from general list
    3. 1 mL sample of LB will be used to measure blank
    4. Take 1 ml sample every hour and measure the cell density
    5. Label the sample with what hour you took it at and spin the sample in the microcentrifuge for 5 minutes
    6. Discard the remaining supernatant (make sure it is all gone) and freeze the pellet
    7. When the OD-reaches between 0.8-1.0 we are ready to induce expression

- **Induction**
    8. We add IPTG to the sample at this point
    9. Need to make a final concentration of 1M. Procedure is as follows
        - Take IPTG out of freezer.
        - Measure out 240 mg (0.24 g).
        - Take 1 ml sample from your culture and place in a microcentrifuge tube.
        - Pour the IPTG into the sample and mix by vortexing.
        - Decant into your culture flask

- Two options at this point
    - 1) If your polymer fractions are unknown then take a sample every hour for 4 hours.
    - 2) If polymer fractions are known take a sample at the end of the induction.

A.2 SDS-PAGE Gel Setup and Running

1. Take 1 ml samples of bacterial culture
2. Pellet bacterial cells by centrifugation at 5,000 RPM for 5 minutes
3. Resuspend the cells in 100 µl B-PER II by vortexing
4. Centrifuge for 5 minutes
5. Collect the supernatant (soluble fraction) and resuspend the pellet (insoluble fraction) in 100 µl of B-PER II.
6. Use 15 µl of each for SDS-PAGE analysis
7. Combine samples with 4X sample buffer
8. Boil at 100 °C for 5 minutes
9. Prepare the gel by washing with dH_20
10. Fill the Mini-Protean gel box with 1X Tris-glycine SDS running buffer
11. Load the gel into the gel box
12. Remove excess bubbling around the gel with disposable pipette
13. Load the sample into the gel using gel loading pipette tips
14. Load the chosen molecular weight marker
15. Close the chamber and set the voltage to 80 V
16. Run for 2-3 hours
17. After it is finished and the gel is extracted from the cassette, wash the gel 3 times for 5 minutes with dH_20.
18. Fill the sample with Blue stain for 2-3 hours with rocking
19. To de-stain pour out stain and fill with dH_20 overnight

A.3 Plasmid Mini-Prep Procedure

1. Spin overnight culture in centrifuge (Dynac Inc.) at max speed for 10-15 minutes.

2. Pour out remaining supernatant and keep pelleted bacterial cells.

3. Resuspend pelleted bacterial cells in 250 µl Buffer P1 by agitating the mixture.

4. Transfer the resuspended pellet to a microcentrifuge tube.

5. Add 250 µl of Buffer P2 and mix thoroughly by inverting the tube gently 4-6 times. The solution should turn blue.

6. Add 350 µl of Buffer N3 and mix immediately and thoroughly by inverting the tube 4-6 times. The solution should be colorless and phase separated.

7. Centrifuge for 10 minutes at 13, 000 RPM in a table-top microcentrifuge (Eppendorf).

8. Apply the supernatant to the QIAprep spin column by pipetting or decanting. Avoid transferring any of the pellet to the spin column.

9. Centrifuge for 1 minute and discard the flow through.

10. Wash the spin column by adding 0.75 ml of Buffer PE and centrifuge for 1 minute. Discard the flow through.

11. Centrifuge for 1 additional minute to remove residual ethanol present in Buffer PE.

12. To elute the DNA place the QIA prep column in a clean 1.5 ml microcentrifuge tube. Add 34 µl of Buffer EB or nuclease free water to the center of the spin column. Let stand for 1 minute and centrifuge for 1 minute.

A. 4 Glycerol Frozen Stocks

1. Take 500 ml of overnight culture and transfer to cryo-vials for storage.
2. Add 500 ml of autoclaved 50% glycerol solution to cryo-vial.
3. Vigorously shake the vial to ensure mixing.
4. Immediately transfer to -80°C freezer for storage.

A.5 1.5 % Agarose Gel Preparation and Operation

1. Add 1.1 g of agarose to a beaker containing 75 ml 1X TAE buffer

2. Stir and heat until boiling occurs

3. Add 7.5 µl ethidium bromide and mix

4. Pour into gel box holder and insert sample combs for well formation

5. Let sit at room temperature for 1-2 hours

6. Remove the combs and place in the gel box

7. Fill the gel box with 1x TAE buffer

8. Run at 80-120V with sample and appropriate marker